Table of Contents

General Information

NMR spectroscopy: NMR spectra were measured on a Bruker Avance II 400 MHz, Avance III 400 MHz HD, Avance III 600 MHz or Avance Neo 700 MHz spectrometer at 25 °C if not otherwise noted. All samples were measured in $CDCl_3$. As the internal reference, the shifts of the solvent residual peaks were used.[1]

Mass spectrometry: MS spectra were measured on a Bruker Impact II. The samples were dissolved in dichloromethane and hexane. All measurements were done in both positive and negative modes. For the positive mode, a positive voltage of 4500 V was applied to the capillary and - 500 V to the End Plate Offset. The nebulizer was set to 0.4 bar. The dry heater was set to 180 °C and the flow of nitrogen as the dry gas to 4.0 l/min. For measurements in the negative ion mode, a negative voltage of 3000 V was applied, while the other parameters remained the same.

Chemicals: The chemicals were purchased from Sigma-Aldrich, Acros Organics, ABCR, Alfa Aesar, BLDPharm and TCI Europe. Anhydrous solvents were purchased from Acros Organics. Deuterated solvents were purchased from Euriso-Top GmbH or deutero. Technical grade solvents, used during work-up and purification, were distilled prior to use.

Column Chromatography: flash column chromatography was carried out with Silica 60 M (0.04 – 0.063 mm) from Macherey-Nagel GmbH & Co. KG. Thin layer chromatography was carried out on Polygram® SIL G/UV254 from Macherey-Nagel GmbH & Co. KG.

Thermogravimetric analysis was conducted on a STA409 PC Luxx thermogravimetric analyzer (Netzsch) over a temperature range from 25 to 700 °C with a heating rate of 10 °C min^{-1} in synthetic air (80% N_2, 20% O_2).

TEM: measurements were carried using a Philips CM30 instrument equipped with a LaB_6 cathode (300 kV). The sample was suspended in DCM and drop cast on carbon-sputtered copper grids (Plano). After drying, the grids were loaded. The particle size was determined by measuring around 350 nanoparticles for each sample. Data were analyzed using the image analysis software ImageJ.

DLS: measurements were performed with a Malvern Zetasizer Nano ZS instrument equipped with a 633 nm He-Ne laser. Samples were dissolved in DCM and filtered with a syringe filter before loading to the cuvette.

SERS: spectra were recorded using a 633 nm HeNe laser (Thor Labs) aligned into an inverted microscope with approximately 6 mW and 600 µW of power at the objective (Nikon, 20x, NA = 0.5) respectively. Backscattered light is passed through a Rayleigh rejection filter (Semrock) prior to detection by a dispersive spectrometer (Acton SP2300, Princeton Instruments, 1200 g/mm). Measurements were taken directly, without prior aggregation with 1M NaBr.

X-ray diffraction was measured with an Empyrean diffractometer (PANalytical) using Cu Kα radiation with 2θ in the range from 35.0° to 90.0° and a step size of 0.02°.

MALDI-MS experiments were carried out using an AP-SMALDI^5 AF (TransMIT GmbH, Giessen, Germany), imaging system (pixel size: ≥5 µm) coupled to a Q Exactive™ HF (Thermo Fisher Scientific (Bremen) GmbH, Germany). All measurements were performed in a positive-

ion mode with Orbital Trapping Mass Spectrometer (for high mass accuracy), and with a high mass resolution of 240,000.

Syntheses of precursors

General procedure for the syntheses of imidazolium compounds.[2]

To a solution of aryl alkyl amine (2.07 eq) in acetic acid/water (3:1 v/v, 20 ml), aqueous formaldehyde (1.00 eq) was added dropwise over 10 min. Then, glyoxal (40% in water, 1.09 eq) was added dropwise over 10 min, and the mixture was stirred at 40 °C for 18h. After the mixture was allowed to cool to rt, hydrochloric acid (1.5 eq, 3 M) was added, and the mixture was heated to 40 °C. After 2h, the reaction was cooled to rt, diluted with 20 mL of water and extracted with DCM. The residue was dried under vacuum at 50 °C to yield the imidazolium compound as a brown oil.

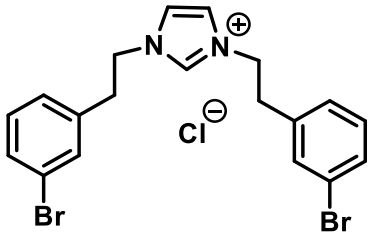

1,3-Bis(3-bromophenethyl)-1*H*-imidazol-3-ium chloride (1d): The General Procedure afforded **1d** as a brown oil (4.00 g, 9.87 mmol, 86%). ^{1}H NMR (400 MHz, $CDCl_3$): δ=10.26 (s, 1H), 7.32-7.30 (m, 6H), 7.16-7.08 (m, 4H), 4.53 (t, *J*=7.4 Hz, 4H), 3.16 (t, *J*=7.4 Hz, 4H) ^{13}C NMR (101 MHz, $CDCl_3$): δ=174.19, 138.39, 137.41, 131.83, 130.65, 127.71, 122.80, 122.27, 50.74, 36.38. HR-MS (ESI): m/z calcd for $C_{19}H_{19}Br_2N_2$: 432.9910, found: 432.9920 (M^+).

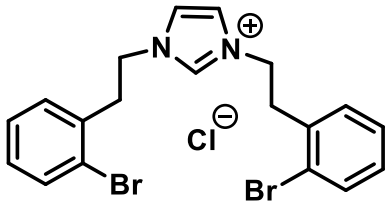

1,3-Bis(2-bromophenethyl)-1*H*-imidazol-3-ium chloride (2d): The General Procedure afforded **2d** as a brown oil (2.33 g, 4.95 mmol, 84%). ^{1}H NMR (400 MHz, $CDCl_3$): δ=10.44 (s, 1H), 7.53-7.51 (m, 2H), 7.32-7.29 (m, 2H), 7.25-7.21 (m, 2H), 7.14-7.09 (m, 2H), 6.93 (d, *J*=1.6 Hz, 2H), 4.60 (t, *J*=7.3 Hz, 4H), 3.36 (t, *J*=7.3 Hz, 4H) ^{13}C NMR (101 MHz, $CDCl_3$): δ=175.41, 138.22, 135.42, 133.05, 131.79, 129.44, 124.43, 121.83, 49.59, 36.95. HR-MS (ESI): m/z calcd for $C_{19}H_{19}Br_2N_2$: 432.9910, found: 432.9905 (M^+).

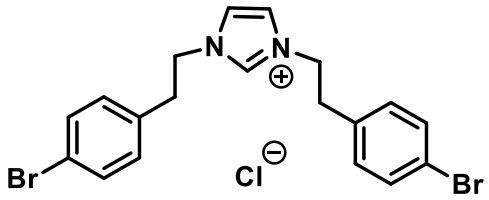

1,3-Bis(4-bromophenethyl)-1*H*-imidazol-3-ium chloride (3d): The General Procedure afforded **3d** as a brown oil (2.20 g, 4.67 mmol, 79%). ^{1}H NMR (400 MHz, $CDCl_3$): δ=10.30 (s, 1H), 7.39-7.36 (m, 4H), 7.08-7.05 (m, 6H), 4.54 (t, *J*=7.2 Hz, 4H), 3.19 (t, *J*=7.2 Hz, 4H). ^{13}C NMR (101 MHz, $CDCl_3$): δ=175.28, 137.81, 134.97, 132.18, 130.72, 121.93, 50.87, 35.93. HR-MS (ESI): m/z calcd for $C_{19}H_{19}Br_2N_2$: 432.9910, found: 432.9907 (M^+).

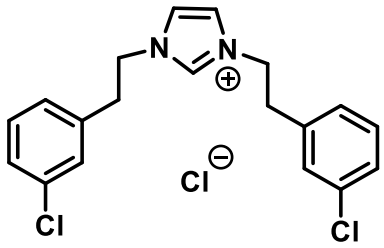

1,3-Bis(3-chlorophenethyl)-1*H*-imidazol-3-ium chloride (4d): The General Procedure afforded **4d** as a brown oil (2.80 g, 7.33 mmol, 97%). ^{1}H NMR (400 MHz, $CDCl_3$): δ=10.47 (s, 1H), 7.22-7.19 (m, 4H), 7.16-7.15 (m, 2H), 7.11-7.08 (m, 4H), 4.57 (t, *J*=7.2 Hz, 4H), 3.19 (t, *J*=7.2 Hz, 4H). ^{13}C NMR (101 MHz, $CDCl_3$): δ=174.60, 137.97, 134.61, 130.39, 128.87, 127.67, 127.19, 121.87, 50.84, 36.18. HR-MS (ESI): m/z calcd for $C_{19}H_{19}Cl_2N_2$: 345.0920, found: 345.0918 (M^+).

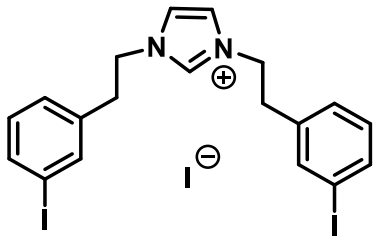

Synthesis of 1,3-bis(3-iodophenethyl)-1*H*-imidazol-3-ium iodide (5d): To a 50 mL 3-neck flask, CuI (14.7 mg, 0.307 eq, 0.0767 mmol), 1,2-dimethyl ethylene diamine (15.9 mg, 0.613 eq, 0.153 mmol), NaI (74.9 mg, 2.00 eq, 0.500 mmol), **1d** (118 mg, 1.00 eq, 0.250 mmol) and anhydrous 1,4-dioxane (5.00 mL) were added under nitrogen flow. The reaction was then heated to 110 °C for 24 h. The mixture was cooled to rt, diluted with water and extracted with EtOAc. The crude mixture was washed thoroughly with acetone and further purified by flash chromatography (silica gel, hexane/ethyl acetate 2:1) to obtain **5d** as a brown sticky solid (20.0 mg, 0.0310 mmol, 12%). ^{1}H NMR (400 MHz, $CDCl_3$): δ=10.24 (s, 1H), 7.59-7.52 (m, 1H), 7.39-7.33 (m, 2H), 7.23-7.17 (m, 5H), 7.07-7.04 (m, 2H), 4.60 (m, 4H), 3.26 (m, 4H). ^{13}C NMR (101 MHz, $CDCl_3$): δ=174.43, 138.94, 131.87, 129.31, 128.98, 127.84, 125.31, 123.07, 51.56, 36.64. HR-MS (ESI): m/z calcd for $C_{19}H_{19}I_2N_2$: 528.9632, found: 528.9629 (M^+).

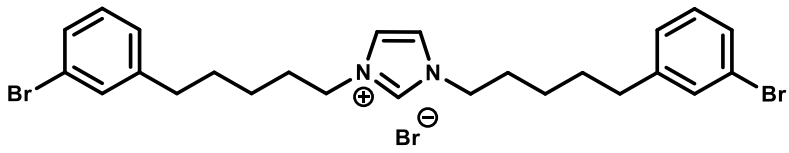

Synthesis of 1,3-bis[5-(3-bromophenyl)pentyl]-1*H*-3λ^4-imidazole (6d): Imidazole (58.3 mg, 2.14 eq, 0.856 mmol) was dissolved in 10 mL THF, and NaH (14.3 mg, 1.42 eq, 0.568 mmol) was added. The mixture was stirred at rt for 30 min. Then, 3-(5-bromopentyl)-1-bromobenzene (122 mg, 1.10 eq, 0.400 mmol) was added. The reaction mixture was heated at 80°C and stirred overnight, then quenched with water, and the mixture was extracted with diethyl ether. The organic layer was separated, dried over Na_2SO_4, and solvent was removed under reduced pressure. The crude product was purified by column chromatography (silica gel, hexane/ethyl acetate 2:1) to give the mono alkylated product as a yellow sticky solid (106 mg, 0.362 mmol 90%). ^{1}H NMR (400 MHz, $CDCl_3$): δ=8.14 (s, 1H), 7.33-7.30 (m, 2H), 7.18-7.06 (m, 3H), 6.97-6.95 (m, 1H), 4.05 (t, *J*=7.2 Hz, 2H), 2.57 (t, *J*=7.6 Hz, 2H), 1.85 (p, *J*=7.8 Hz, 2H), 1.64 (m, 2H), 1.38-1.30 (m, 2H). ^{13}C NMR (101 MHz, $CDCl_3$): δ=144.50, 136.95, 131.51, 130.08, 129.14, 128.71, 127.16, 122.50, 119.03, 47.30, 35.45, 31.01, 30.76, 26.18. HR-MS (ESI): m/z calcd for $C_{14}H_{17}BrN_2$: 292.0575, found: 293.0644 $(M+H)^+$.

To a solution of the mono alkylated product (53.0 mg, 1.00 eq, 0.190 mmol) in toluene, 3-(5-bromo pentyl)-1-bromo benzene (64.0 mg, 1.10 eq, 0.209 mmol) was added, and the mixture was stirred at 90 °C for 6d. The completion of the reaction was marked by the crashing out of solid, which was diluted with water, extracted with CH_2Cl_2 and precipitated with acetone to obtain the imidazolium salt as a brown sticky solid (867 mg, 0.145 mmol, 76%). ^{1}H NMR (400 MHz, $CDCl_3$): δ=10.96 (s, 1H), 7.32-7.28 (m, 4H), 7.17-7.09 (m, 6H), 4.34 (t, *J*=7.5 Hz, 4H), 2.59 (t, *J*=7.5 Hz, 4H), 1.95 (p, *J*=7.6 Hz, 4H), 1.67 (p, *J*=7.5 Hz, 4H), 1.40 (m, 4H). ^{13}C NMR (101 MHz, $CDCl_3$): δ=182.37, 144.35, 138.40, 131.53, 129.16, 127.35, 122.52, 121.39, 50.24, 35.24, 30.46, 30.22, 25.70. HR-MS (ESI): m/z calcd for $C_{25}H_{31}Br_2N_2$: 517.0854, found: 517.0850 (M^+).

General procedure for the syntheses of carbene complexes.[3–5]

We observed an unsual behaviour of the Au complexes studied in this work. During the course of purification, there was a scrambling/disproportionation of the complex between Au^+ and Au^{3+} which was made manifest by separation of the aliphatic signals after the syntheses of the complexes and the same phenomenon was found for all the other complexes when left overtime. This scrambling reaction is already literature-known and its mechanism is explicitly described by Gust and coworkers.[6] Similarly, Johnson and coworkers observed a disproportionation of NHC-Au complexes and could only isolate a mixture of both Au^+ and Au^{3+} complexes which were evident in both NMR and MALDI studies.[7] This observation in our present study raised a suspicion of how fast the scrambling occurs with our complexes. For this reason, we tested a series of compound **1e** by preparing and measuring the NMR immediately after the synthesis (that is, without further purification) and compared the NMR spectrum with that taken after 1h, 2d and 6 months of preparation. We could clearly see a separation of the signals in the aliphatic region (after 1h of synthesis), which was found wanting in the NMR taken immediately after the reaction, thus, suggesting a disproportionation between Au^+ and Au^{3+} of these complexes when left overtime (Figure S1). In addition, mass spectra of the complex taken after 6 months of preparation showed the masses of both NHC-Au-Cl and NHC-$AuCl_3$ supporting the disproportionation of these complexes into Au^+ and Au^{3+}, thus, prompting us to use these complexes immediately for the next reaction step and without further purification. It is noteworthy to mention that Au^{3+} is more reactive than Au^+, even when the latter is oxidized to the former, it will still disproportionate to Au^+ which is relatively more stable than Au^{3+}.[8] Our attempts to use the complexes as pure Au^+ species involve using it immediately for the next step without further purification, as this is the only way to ensure no waiting time which is required for the disproportionation reaction. On a side note, it is also important to mention that both the Au^+ and Au^{3+}complexes will eventually give rise to the Nps provided that they are reduced with $NaBH_4$.[9]

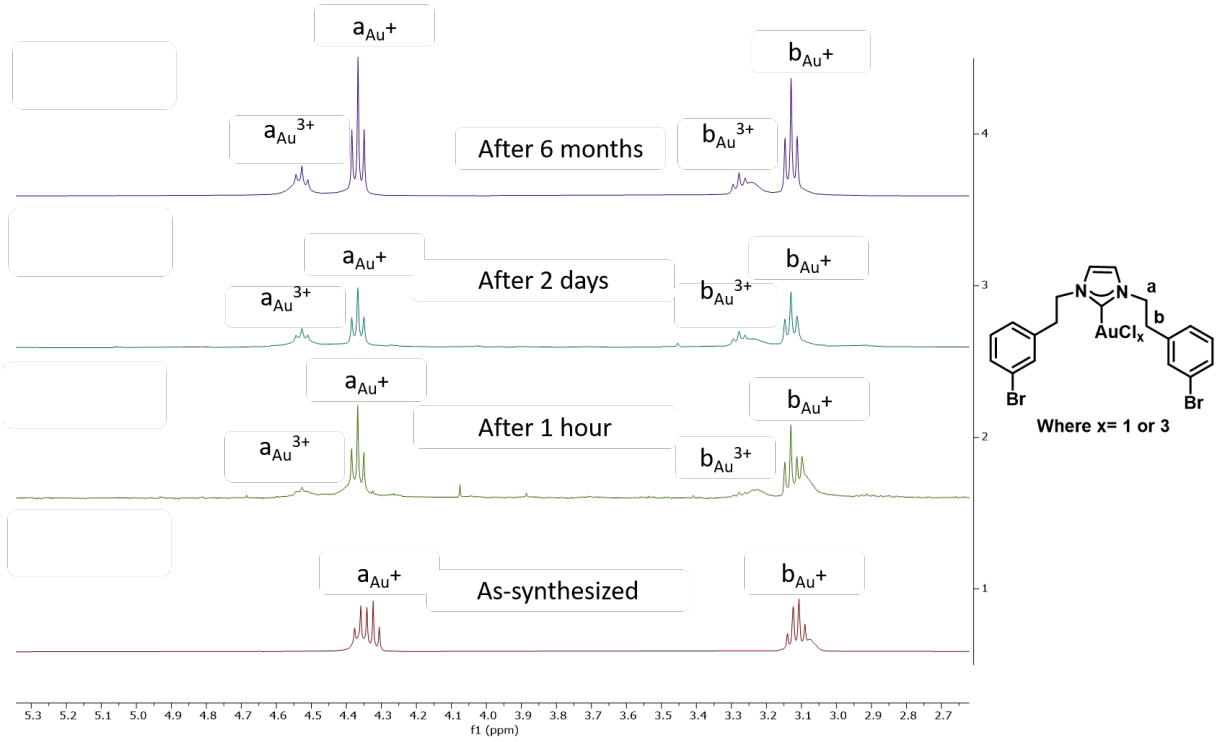

Figure S1. Comparison of the NMR of the as-synthesized complex (**1e**) with that measured after 1h, 2d and 6 months of reaction time, indicating a disproportionation to Au^{3+} when left overtime.

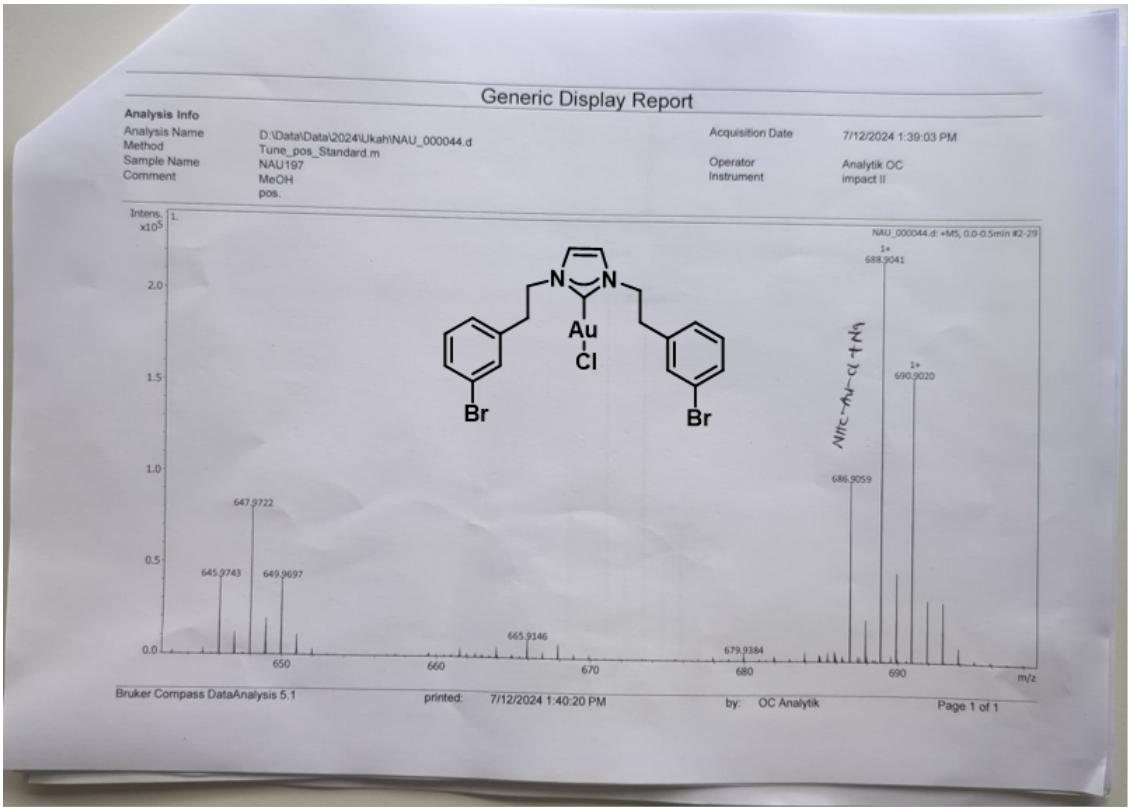

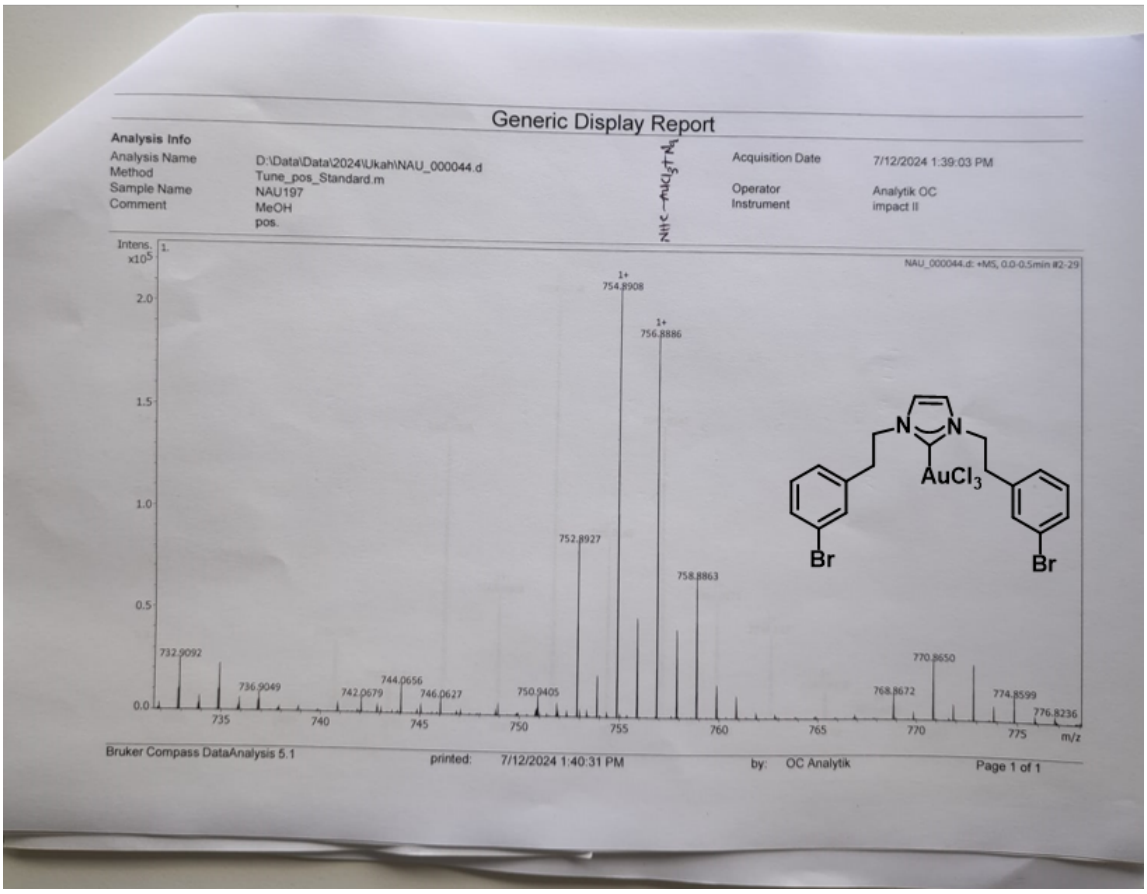

Figure S2. Mass spectrum of **1e** showing both Au^{+} and Au^{3+}. Top spectrum showed Au^{+} fragmentation (NHC-Au-Cl+Na) with a mass peak at 686.9059 (calcd. 686.9077) and bottom spectrum showed Au^{3+} fragmentation (NHC-$AuCl_3$+Na) with a mass peak at 756.85 (calcd. 756.88). Samples were measured 6 months after the synthesis.

Imidazolium salt (1.00 eq, 0.165 mmol), chloro(dimethylsulfide)gold(I) (50.0 mg, 1.00 eq, 0.165 mmol), and K_2CO_3 (68.0 mg, 3.00 eq, 0.490 mmol) were stirred in acetone (15 mL) at 60 °C for 18 h. After cooling to rt, the mixture was filtered through a pad of Celite and acetone was removed under reduced pressure. In the case of purified complexes used for test reactions: the obtained solid was washed with Et_2O to remove any free gold complex followed by precipitation with *n*-pentane, to afford the bound amphiphilic NHC-Au^I complex as a yellow sticky solid.

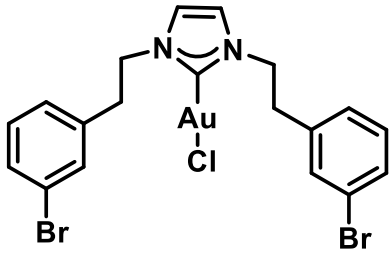

[1,3-Bis(3-bromophenethyl)-2,3-dihydro-1*H*-imidazol-2-yl]gold(I) chloride (1e): The General Procedure afforded **1e** as a yellow sticky solid (80.0 mg, 0.120 mmol, 73%). ^{1}H NMR (400 MHz, $CDCl_3$): δ=7.38-7.29 (m, 2H), 7.21-7.02 (m, 6H), 6.53 (s, 2H), 4.34 (m, 4H), 3.11 (m, 4H). ^{13}C NMR (101 MHz, $CDCl_3$): δ=183.22, 139.63, 131.93, 130.69, 130.46 127.72, 122.88, 120.78, 52.69, 41.88. HR-MS (ESI): m/z calcd for $C_{19}H_{18}AuBr_2ClN_2Na$: 686.9077, found: 686.9084 $(M+Na)^+$.

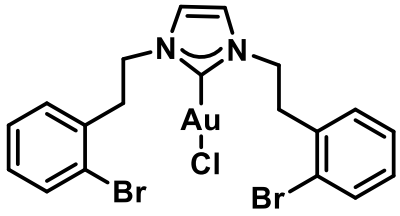

[1,3-Bis(2-bromophenethyl)-2,3-dihydro-1*H*-imidazol-2-yl]gold(I) chloride (2e): The General Procedure afforded **2e** as a yellow sticky solid (70.0 mg, 0.110 mmol, 64%). ^{1}H NMR (400 MHz, $CDCl_3$): δ=7.57-7.45 (m, 2H), 7.24-7.04 (m, 6H), 6.62, (m, 2H), 4.40 (m, 4H), 3.27 (m, 4H). ^{13}C NMR (101 MHz, $CDCl_3$): δ=136.27, 136.18, 133.12, 131.34, 128.02, 124.55, 120.62, 50.90, 37.96. HR-MS (ESI): m/z calcd for $C_{19}H_{18}AuBr_2ClN_2Na$: 686.9077, found: 686.9077 $(M+Na)^+$.

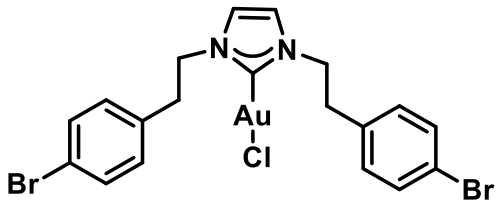

[1,3-Bis(4-bromophenethyl)-2,3-dihydro-1*H*-imidazol-2-yl]gold(I) chloride (3e): The General Procedure afforded **3e** as a yellow sticky solid (90.0 mg, 0.140 mmol, 82%). ^{1}H NMR (400 MHz, $CDCl_3$): δ=7.42-7.31 (m, 4H), 7.05 (m, 4H), 6.46 (s, 2H), 6.49 (m, 1H), 4.33 (m, 4H), 4.17 (m, 4H). ^{13}C

NMR (101 MHz, $CDCl_3$): δ=136.17, 135.69, 131.97, 130.56, 121.93, 52.54, 36.98. HR-MS (ESI): m/z calcd for $C_{19}H_{18}AuBr_2ClN_2Na$: 686.9077, found: 686.9079 $(M+Na)^+$.

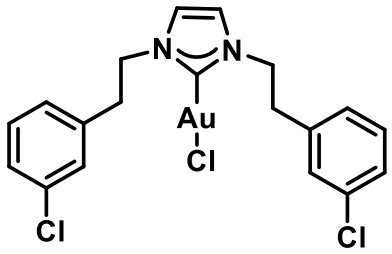

[1,3-Bis(3-chlorophenethyl)-2,3-dihydro-1*H*-imidazol-2-yl]gold(I) chloride (4e): The General Procedure afforded **4e** as a yellow sticky solid (90.0 mg, 0.160 mmol, 95%). ^{1}H NMR (400 MHz, $CDCl_3$): δ=7.59-7.00 (m, 8H), 6.47-6.51 (m 2H), 4.55-4.35 (m, 4H), 3.30-3.12 (m, 4H). ^{13}C NMR (101 MHz, $CDCl_3$): δ=138.92, 134.70, 130.42, 129.03, 127.56, 127.25, 120.73, 52.73, 37.41. HR-MS (ESI): m/z calcd for $C_{19}H_{18}AuCl_3N_2Na$: 599.0094, found: 599.0094 $(M+Na)^+$.

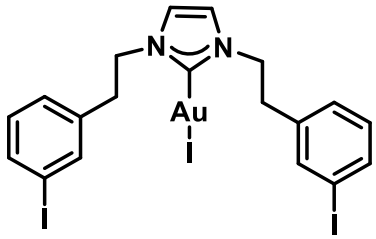

[1,3-Bis(3-iodophenethyl)-2,3-dihydro-1*H*-imidazol-2-yl]gold(I) iodide (5e): The General Procedure afforded **5e** as a yellow sticky solid (20.0 mg, 0.0240 mmol, 76%). ^{1}H NMR (400 MHz, $CDCl_3$): δ=7.59-7.00 (m, 8H), 6.55 (s, 2H), 4.38 (m, 4H), 3.14 (m, 4H). ^{13}C NMR (101 MHz, $CDCl_3$): δ=154.29, 145.51, 139.22, 131.92, 130.78, 127.76, 120.53, 52.41, 37.44. HR-MS (ESI): m/z calcd for $C_{19}H_{18}AuI_2N_2$: 724.9219, found: 724.9225 $(M-I)^-$.

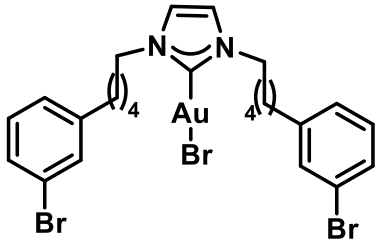

(1,3-Bis(5-(3-bromophenyl)pentyl)-1H-3λ^4-imidazol-2-yl)gold(I) bromide (6e): the General Procedure afforded **6e** as a yellow sticky solid (30.0 mg, 0.0380 mmol, 37%). ^{1}H NMR (400 MHz, $CDCl_3$): δ=7.54 (m, 1H), 7.32 (m, 2H), 7.17-7.05 (m, 6H), 6.88 (s, 1H), 4.19-4.12 (m, 4H), 2.60-2.55 (m, 4H), 1.94-1.82 (m, 4H), 1.66 (m, 4H), 1.34 (m, 4H). ^{13}C NMR (101 MHz, $CDCl_3$): δ=145.11, 131.42, 130.14, 129.09, 127.35, 122.52, 120.37, 51.36, 35.39, 31.07, 30.68, 25.90. HR-MS (ESI): m/z calcd for $C_{25}H_{30}AuBr_3N_2Na$: 814.9517, found: 814.9520 $(M+Na)^+$.

General procedure for the syntheses of AuNps.[4,5,10]

The Au^1-complex (50.0 mg, 1.00 eq, 0.0750 mmol) was dissolved in DCM (10 mL) in a 50 mL round-bottom flask. In a separate vial, $NaBH_4$ (28.4 mg, 10.0 eq, 0.750 mmol) was dissolved in deionized water (10 mL). Immediately, the $NaBH_4$ solution was then added to the gold complex solution and the resulting mixture was vigorously stirred for 18 h at rt. The organic layer was then separated, dried under vacuum and washed with THF to afford the functionalized AuNps as a wine-red solid.

General procedure for Ullmann coupling of AuNps.[10]

In a 5 mL Schlenk flask, NHC-AuNp (20.0 mg), and K_2CO_3 (76.1 mg), were mixed in 0.500 ml DMF and stirred at 120 °C under N_2 for 3 d. The reaction mixture was diluted with water and extracted with DCM. The organic layer was washed several times with water and dried over anhydrous $MgSO_4$. The solvent was evaporated and the resulting colloidal solid was characterized with ATR-IR and SERS.

TEM micrographs

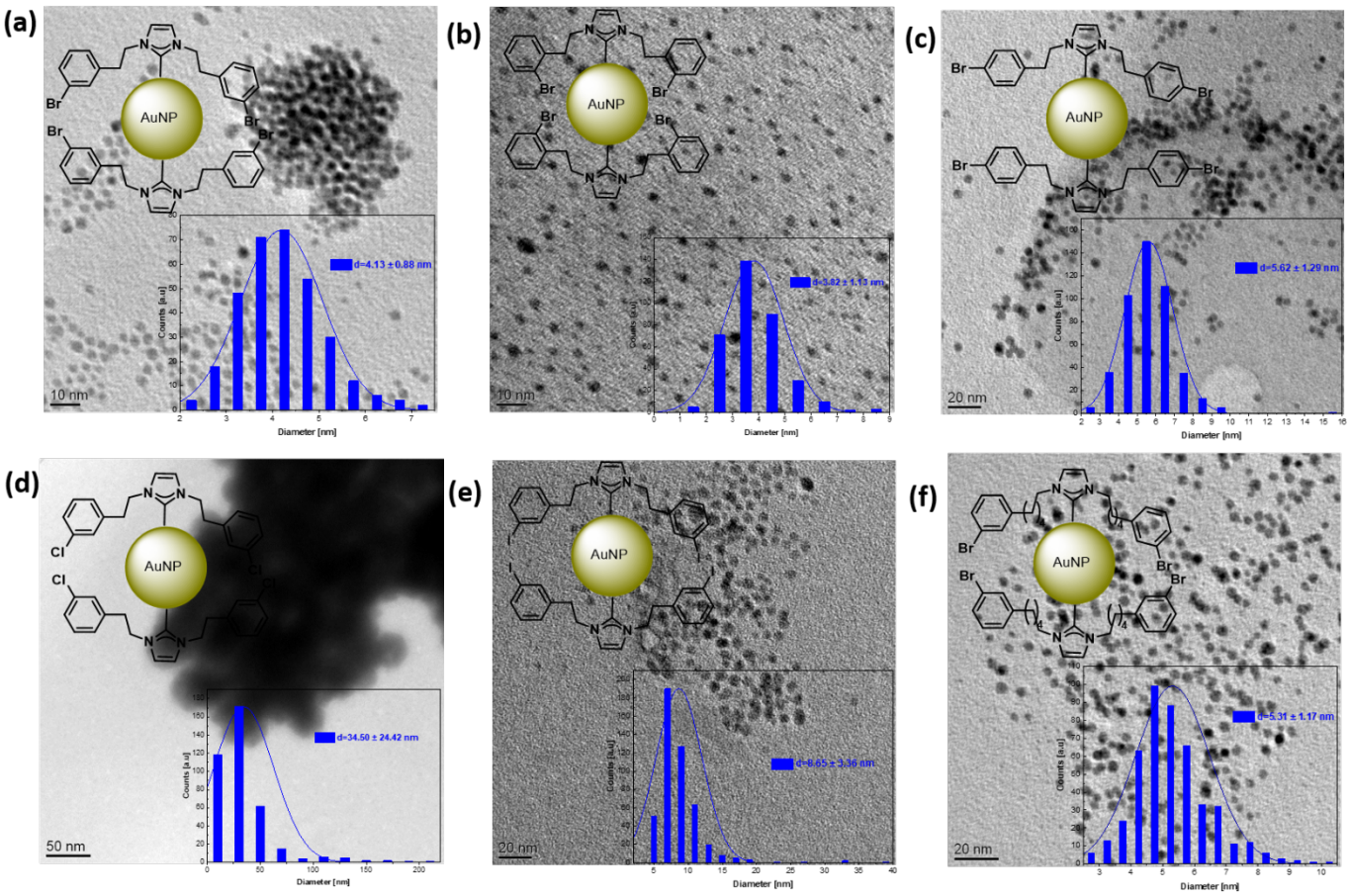

Figure S3: TEM and size distribution (inset) of all functionalized AuNps. (a) **1f-AuNp** with average diameter of 4.10 $\pm$ 0.88 nm. (b) **2f-AuNp** with average diameter of 3.82 $\pm$ 1.13 nm. (c) **3f-AuNp** with average diameter of 5.62 $\pm$ 1.29 nm. (d) **4f-AuNp** with average diameter of 34.5 $\pm$ 24.4 nm. (e) **5f-AuNp** with average diameter of 8.65 $\pm$ 3.36 nm and (f) **6f-AuNp** with average diameter of 5.31 $\pm$ 1.17 nm. Analyses were made with *n*-number of nanoparticles, where $n \geq 400$ depending on the visualization of each functionalized AuNps.

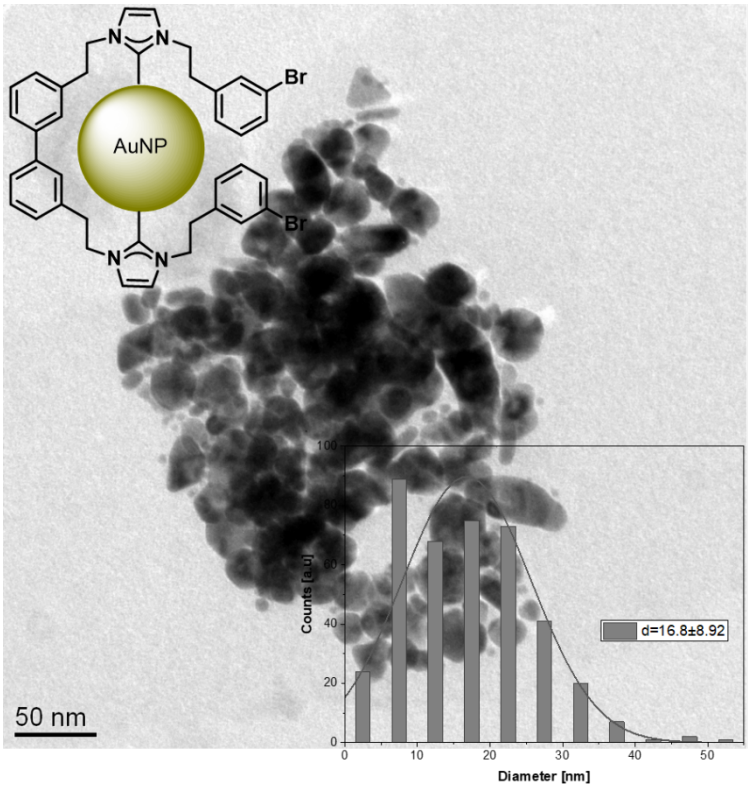

Figure S4: TEM and size distribution (inset) of AuNp after reaction (that is, **1g-AuNp**), with an average core diameter of 16.8±8.92 indicating retention of nanoparticles after on-surface Ullmann reaction.

DLS spectra

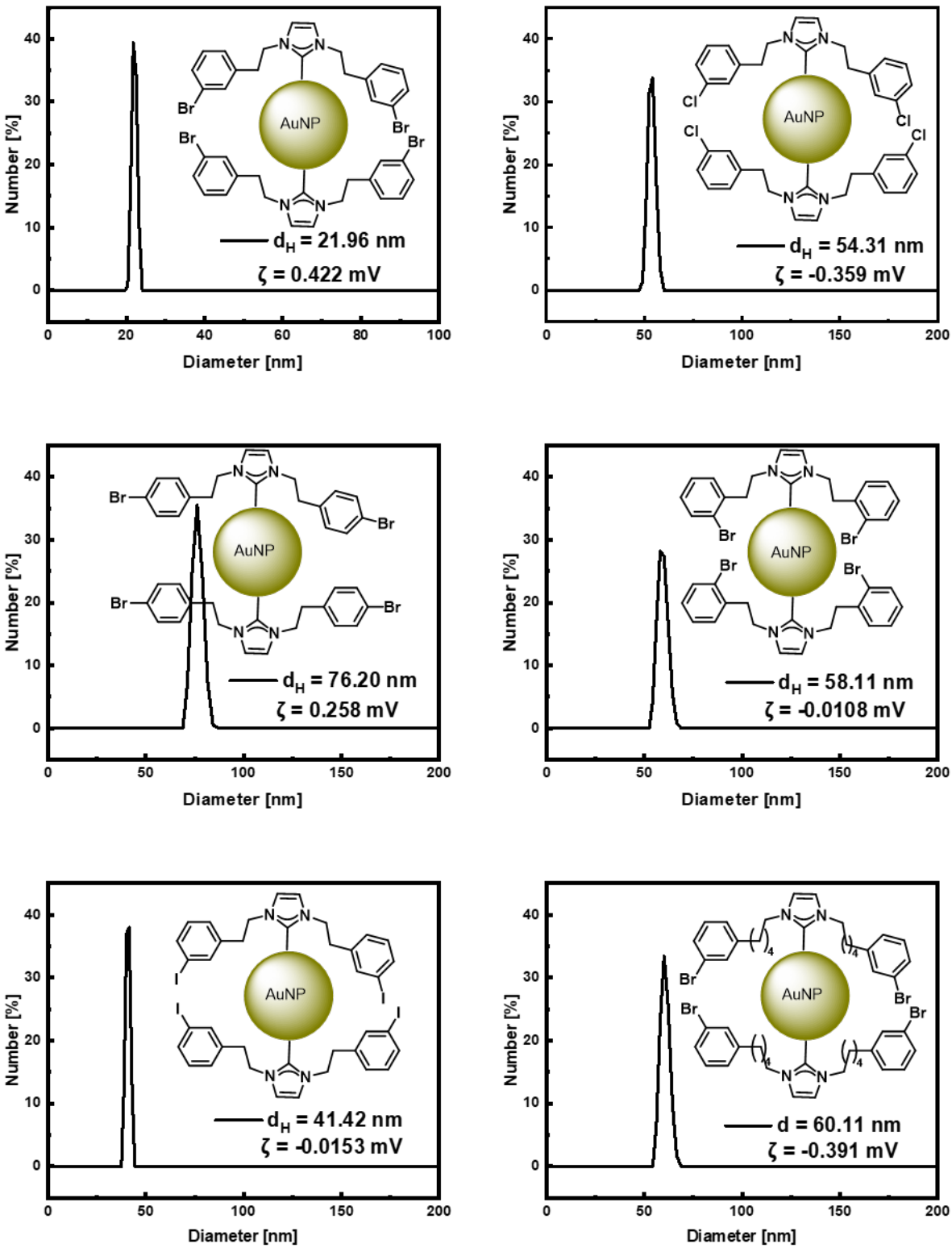

Figure S5: DLS spectra of all functionalized AuNps with their zeta potential values, indicating a neutrality of the AuNps.

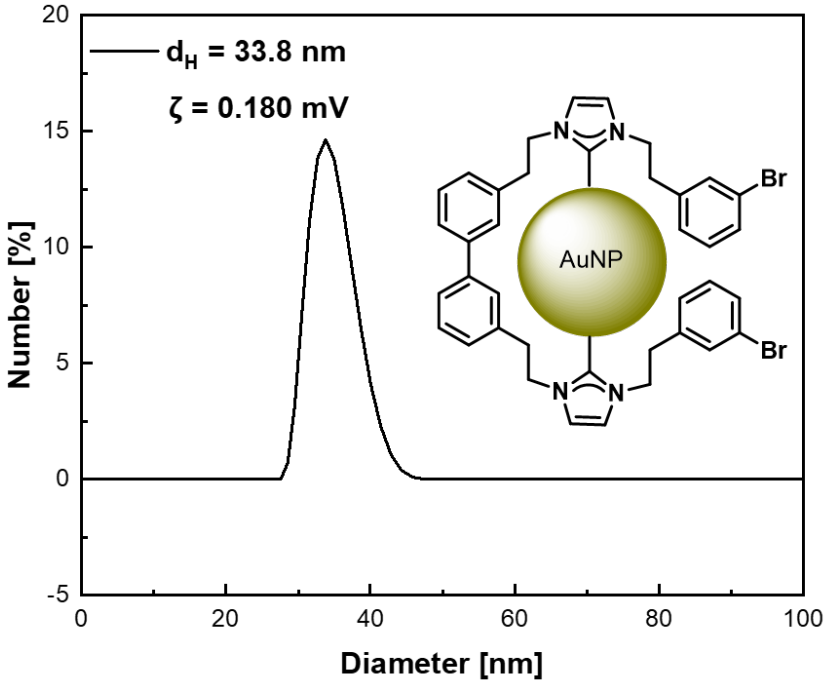

Figure S6: DLS spectrum of **1g-AuNp** with a hydrodynamic diameter of 33.8 nm indicating a retention of nanoparticles after on-surface Ullmann reaction. The compound has a zeta potential of 0.180 mV, indicating a neutrarily charged nanoparticle with a tendency of flocculation when dispersed in DCM.

Energy Dispersive X-ray Spectroscopy (EDX)

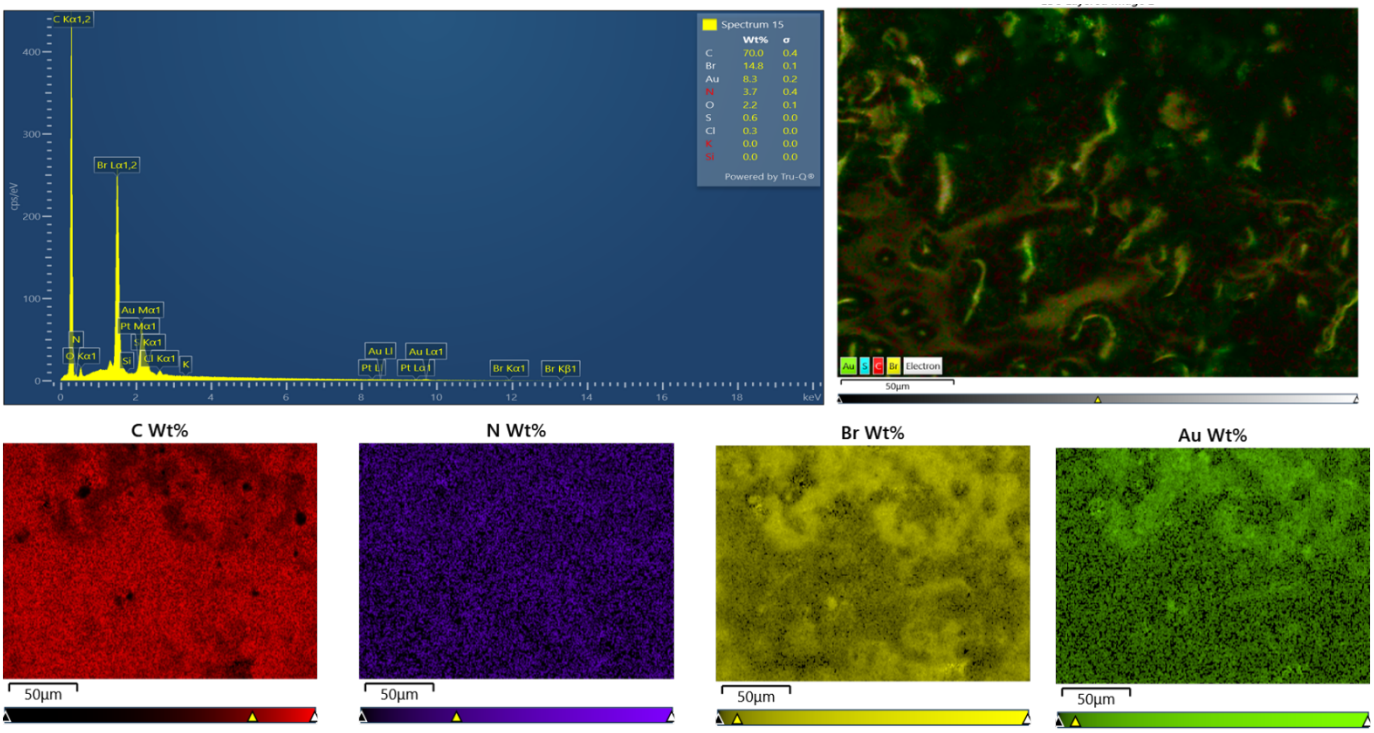

Figure S7: EDX analysis and EDX mapping images of the AuNps before reaction (that is **1f-AuNp**).

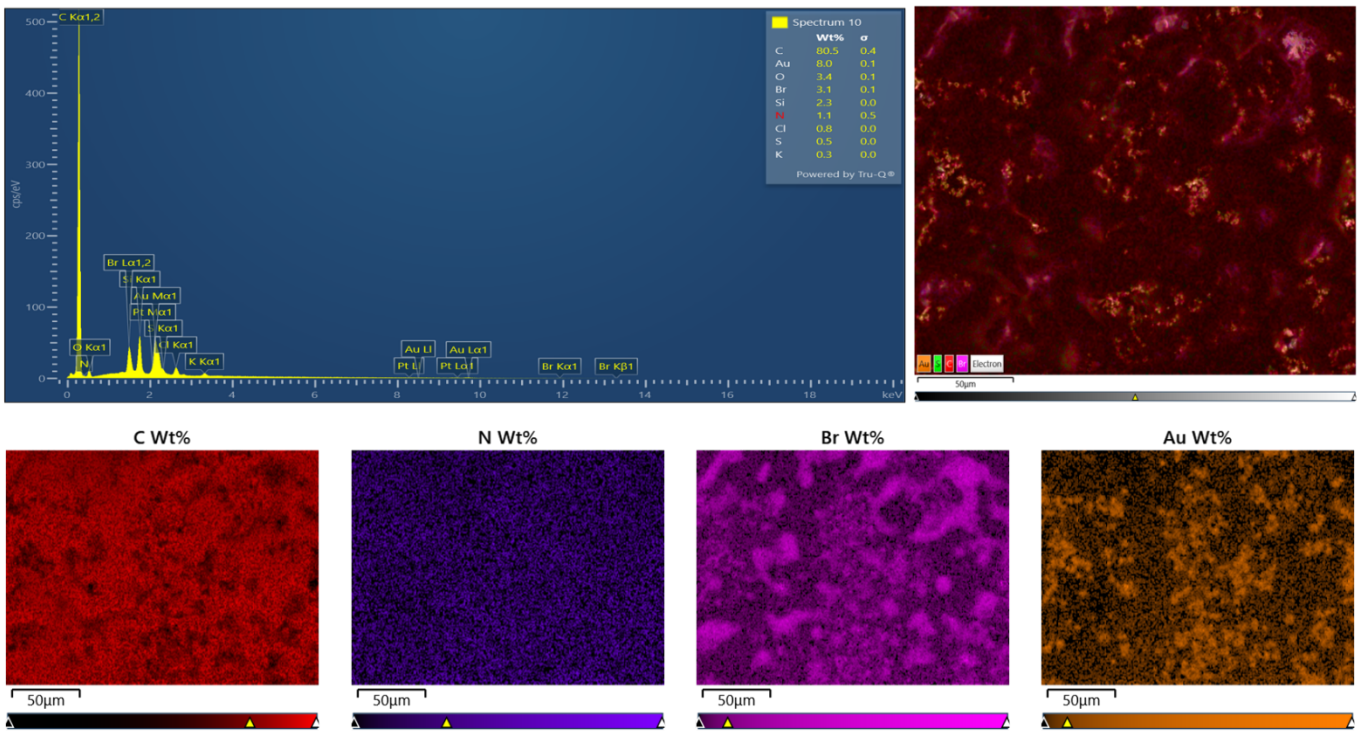

Figure S8: EDX analysis and EDX mapping images of the AuNps after reaction (that is **1g-AuNp**).

Table S1: Comparison of elemental composition obtained from EDX analysis.

Elements	Before reaction(%)	After reaction (%)	Difference (%)
C	70.0	80.5	10.5
Au	8.3	8.0	0.3
Br	14.3	3.1	11.7

XRD

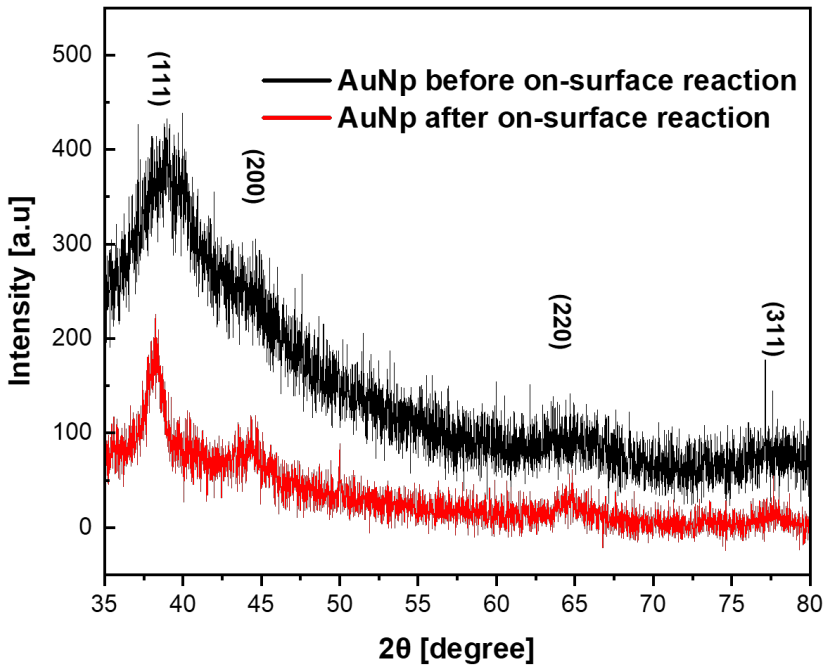

Figure S9: XRD profiles of the AuNps before reaction (**1f-AuNp**) and after reaction (**1g-AuNp**). Note that the sizes of the Nps increased after the reaction, resulting to more pronounced gold reflexes in the XRD profile, since within this size regime, reflexes due to gold start becoming more enhanced.

MALDI-MS

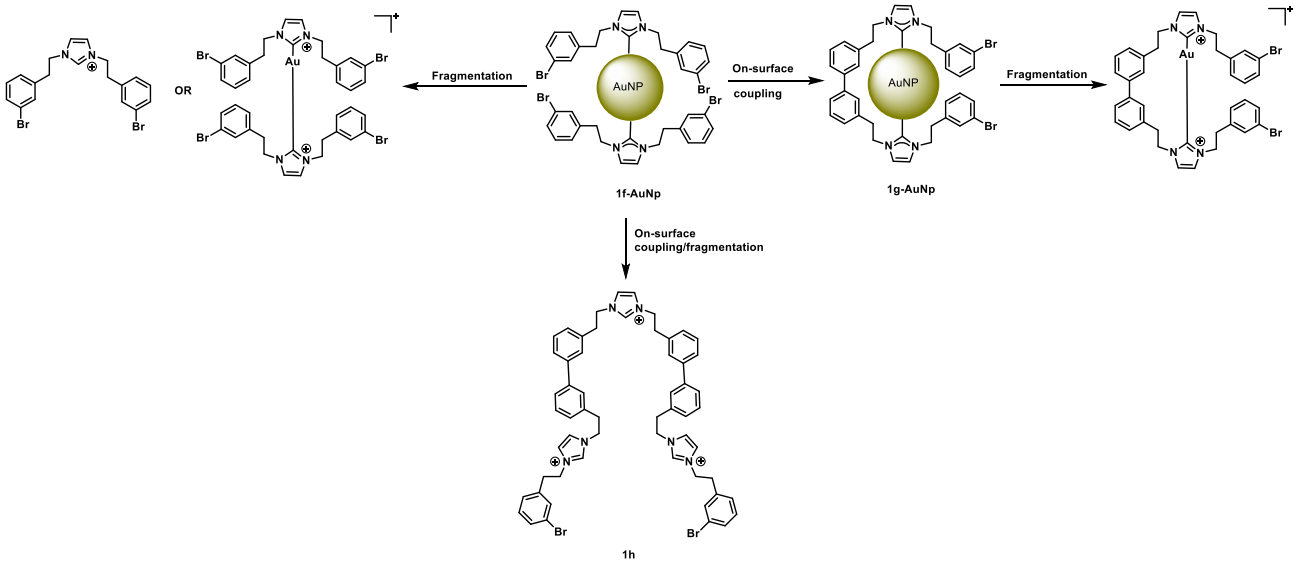

Scheme S1. Reaction scheme and fragmentations for On-surface coupling reactions.

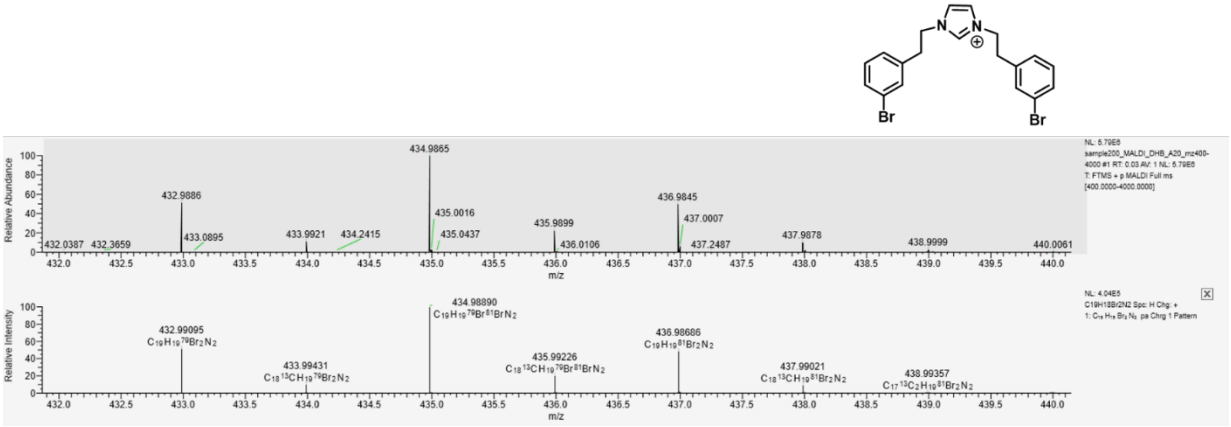

Figure S10: MS spectra of **1f-AuNp**, bottom spectrum (simulated mass spectrum) and top, (experimental mass spectrum). Spectra showed a mass peak at 433.9921 (calc. 433.9943), corresponding to $(MH)^+$ fragmentation.

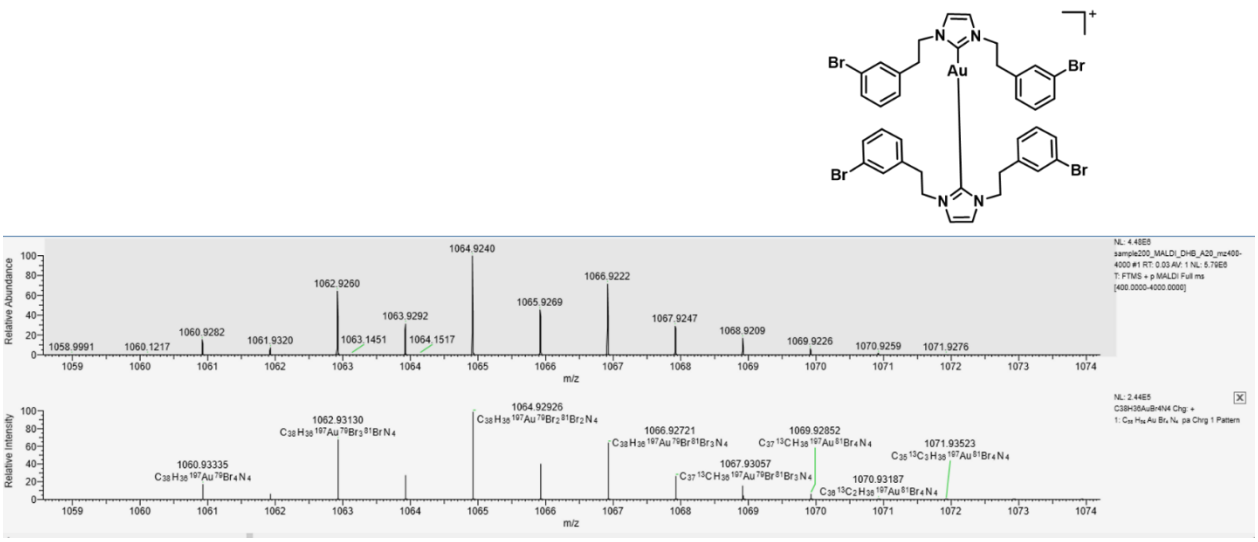

Figure S11: MS spectra of **1f-AuNp**, bottom spectrum (simulated mass spectrum), and top (experimental mass spectrum). Spectra showed a mass peak at 1060.9282 (calc. 1060.9333), corresponding to $(NHC)_2Au^+$ fragmentation, indicating that we have the ligands attached to the AuNps.

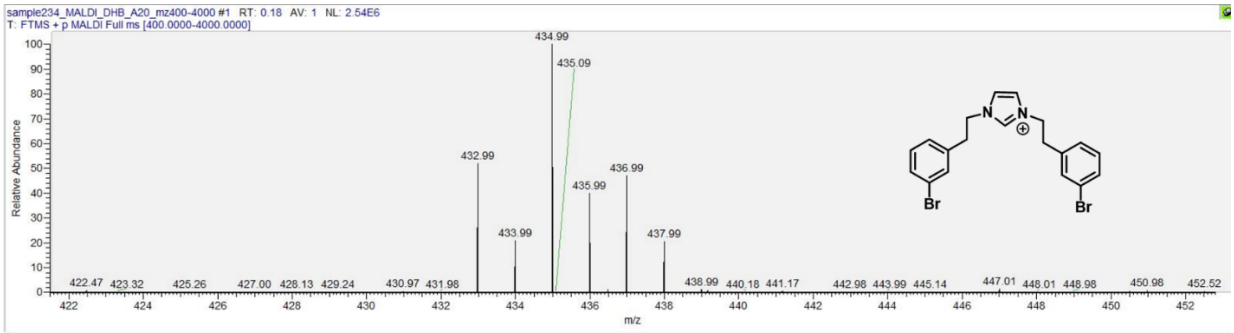

Figure S12: MS spectrum of **1g-AuNp** with a mass peak at 432.99, corresponding to the starting material (**1f-AuNp)**, thus, indicating that the starting material still coexists as a ligand on the surface of the AuNp. This same mass was observed from ESI-MS, on the section, 'synthesis of precursors'.

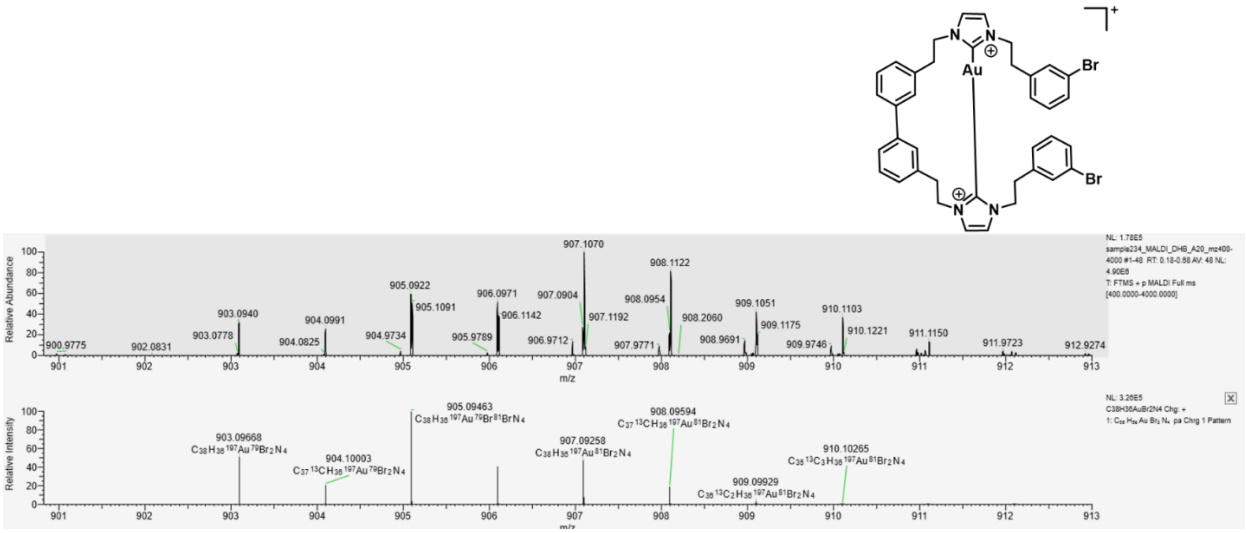

Figure S13: MS spectra of **1f-AuNp**, bottom spectrum (simulated mass spectrum), and top (experimental mass spectrum). Spectra showed a mass peak at 903.0940 (calc. 903.0966), corresponding to the reacted $(NHC)_2Au^+$ fragmentation, indicating that we successfully attained an on-surface functionalization.

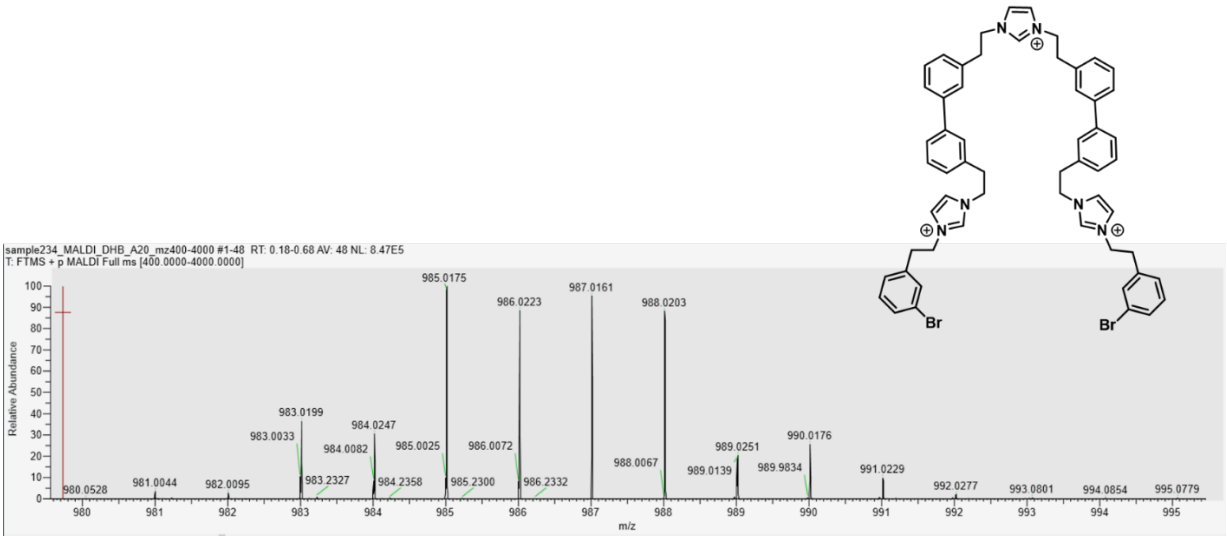

Figure S14: MS spectrum of **1f-AuNp**, with a mass peak at 983.23 (calc. 983.29), corresponding to two coupled units and two open units. This alludes to the so many coupling possibilities attainable, and also confirms our on-surface synthesis.

ATR-IR spectra

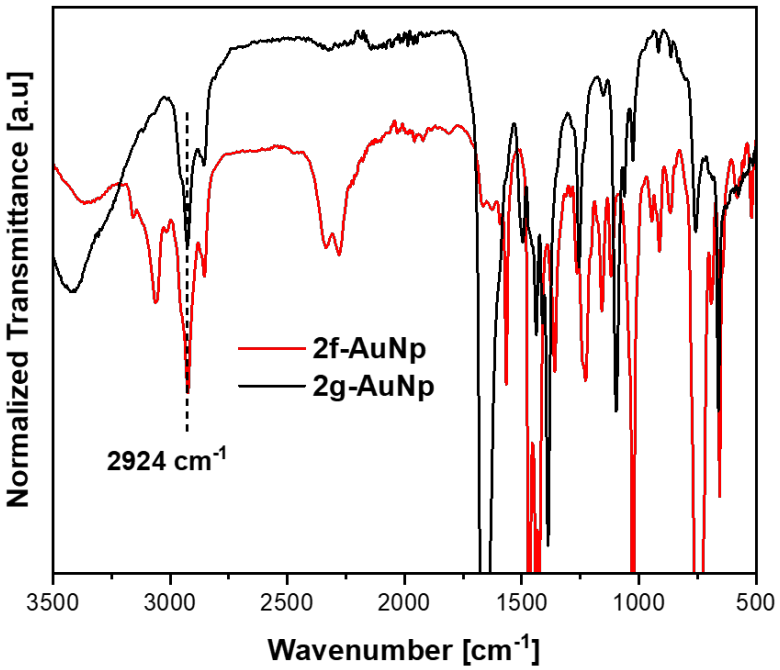

Figure S15: IR spectra of **2f-AuNp** and **2g-AuNp**. Note that all spectra were normalized to 1, using the C-H stretching IR band at 2924 cm^{-1}.

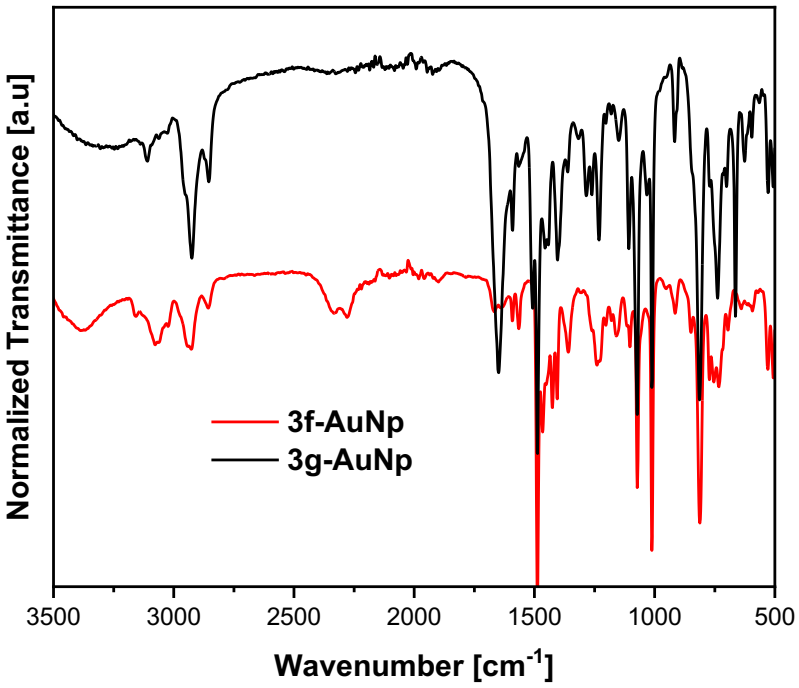

Figure S16: IR spectra of **3f-AuNp** and **3g-AuNp**.

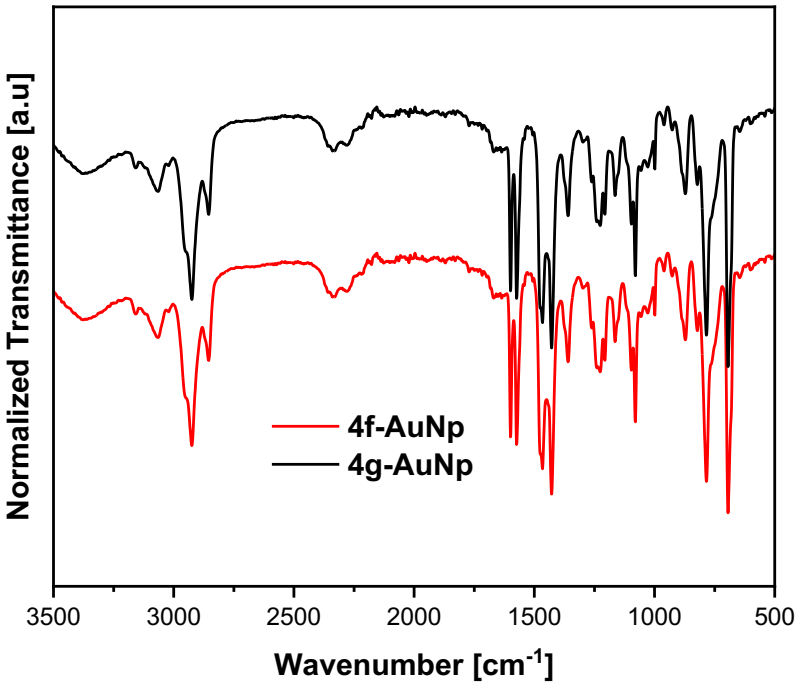

Figure S17: IR spectra of **4f-AuNp** and **4g-AuNp**.

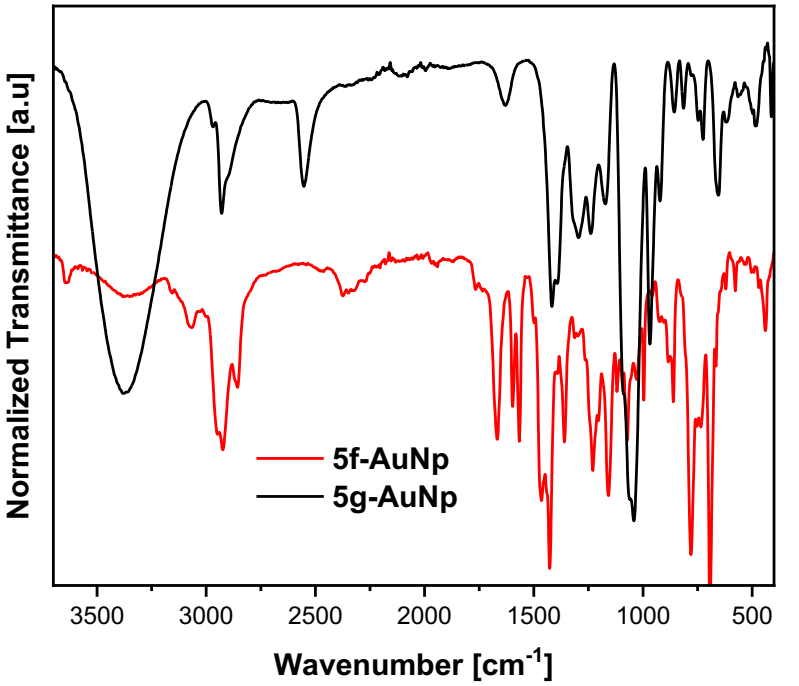

Figure S18: IR spectra of **5f-AuNp** and **5g-AuNp**, with signficant brodenings and appearance of new bands suggesting possible decomposition of the starting material.

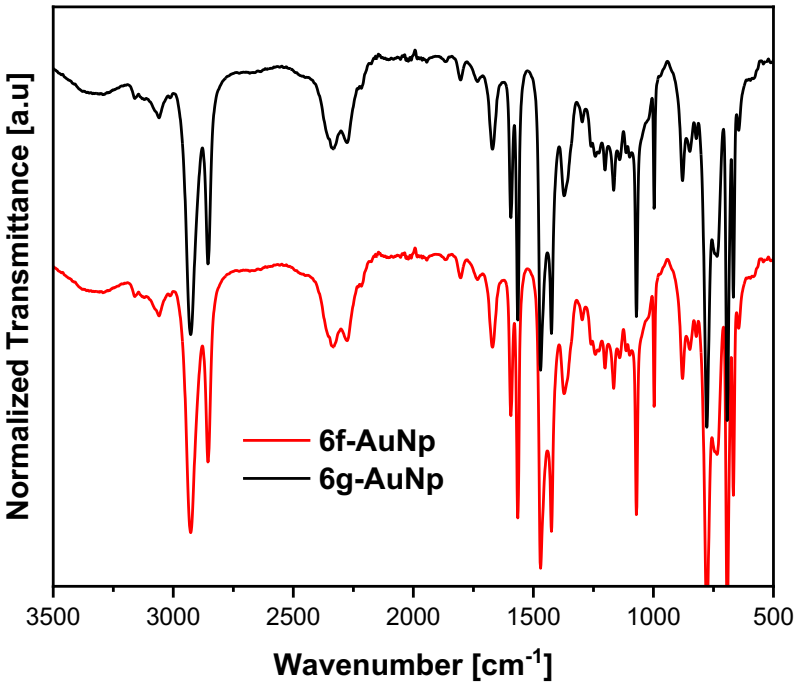

Figure S19: IR spectra of **6f-AuNp** and **6g-AuNp**.

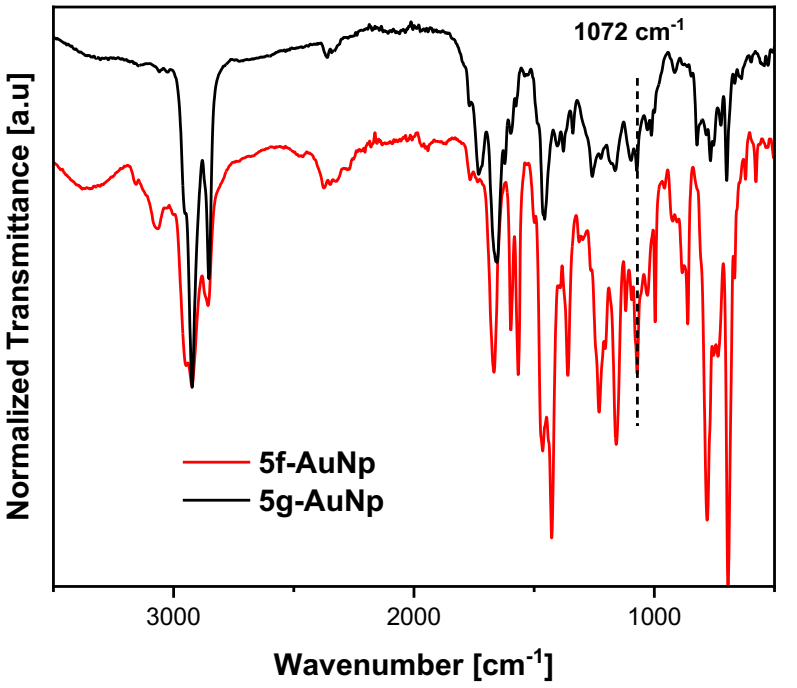

Figure S20: IR spectra of **5f-AuNp** and **5g-AuNp** synthesized at 100 °C. Note that Iodine is heavier than Bromine and therefore, the stretch occurs at a slightly different wavenumber from the C-Br stretch.

SERS spectra

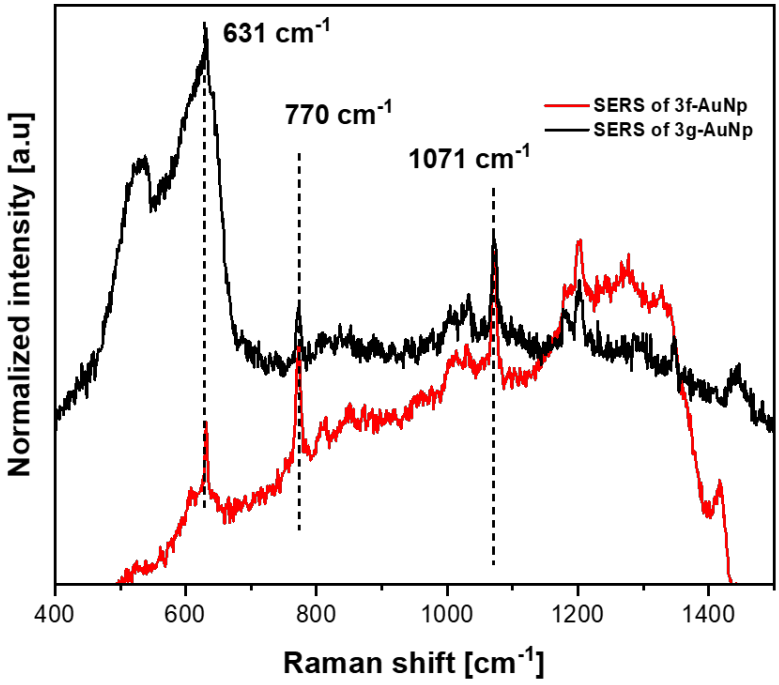

Figure S21: SERS spectra of **3f-AuNp** and **3g-AuNp**, showing retention of starting material with bands at 631, 770 and 1071 cm^{-1}, corresponding to C-Br, C-C aliphatic wingtip groups and benzene units. Thus, suggesting a high degree of stabilty and suitability of this compound for surface stabilization but unsuitable for surface functionalization.

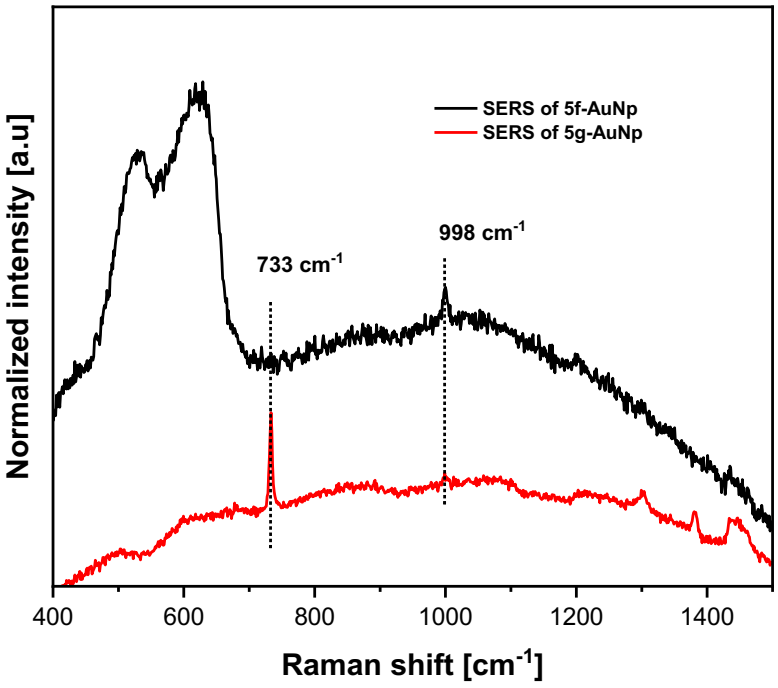

Figure S22: SERS spectra of **5f-AuNp** and **5g-AuNp**, showing an intensification of C-C aliphatic chains due to band at 733 cm^{-1}, relative to the starting material, **5f-AuNp**. There was a slight retention of aromatic rings at 998 cm^{-1}, which is suggestive of a decomposition of the starting material at the temperature of reaction

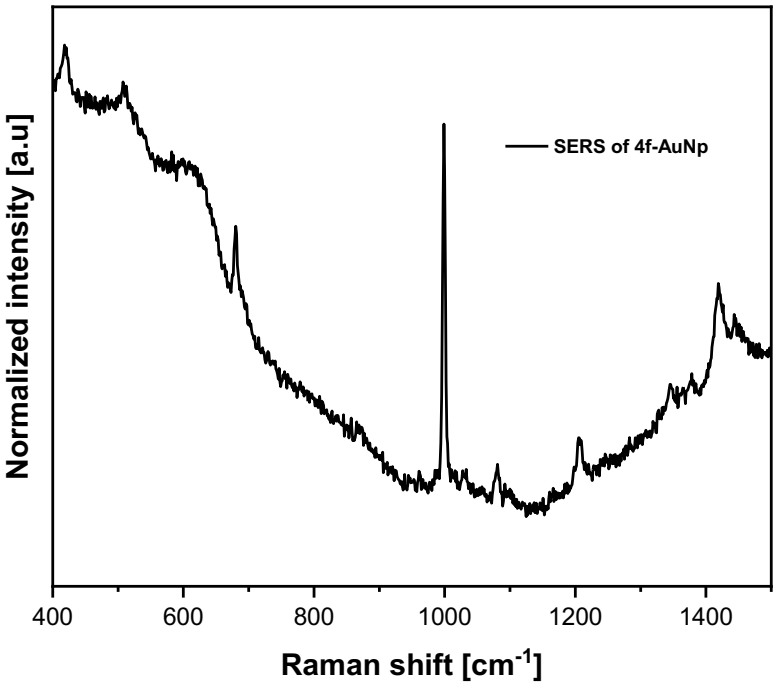

Figure S23: SERS spectra of **4f-AuNp**.

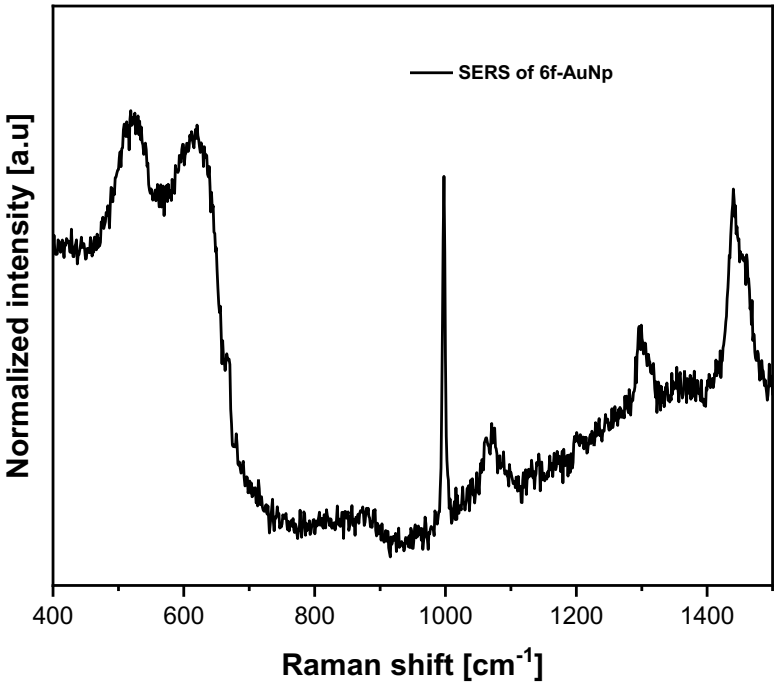

Figure S24: SERS spectra of **6f-AuNp**.

NMR spectra

1,3-Bis(3-bromophenethyl)-1*H*-imidazol-3-ium chloride (1d)

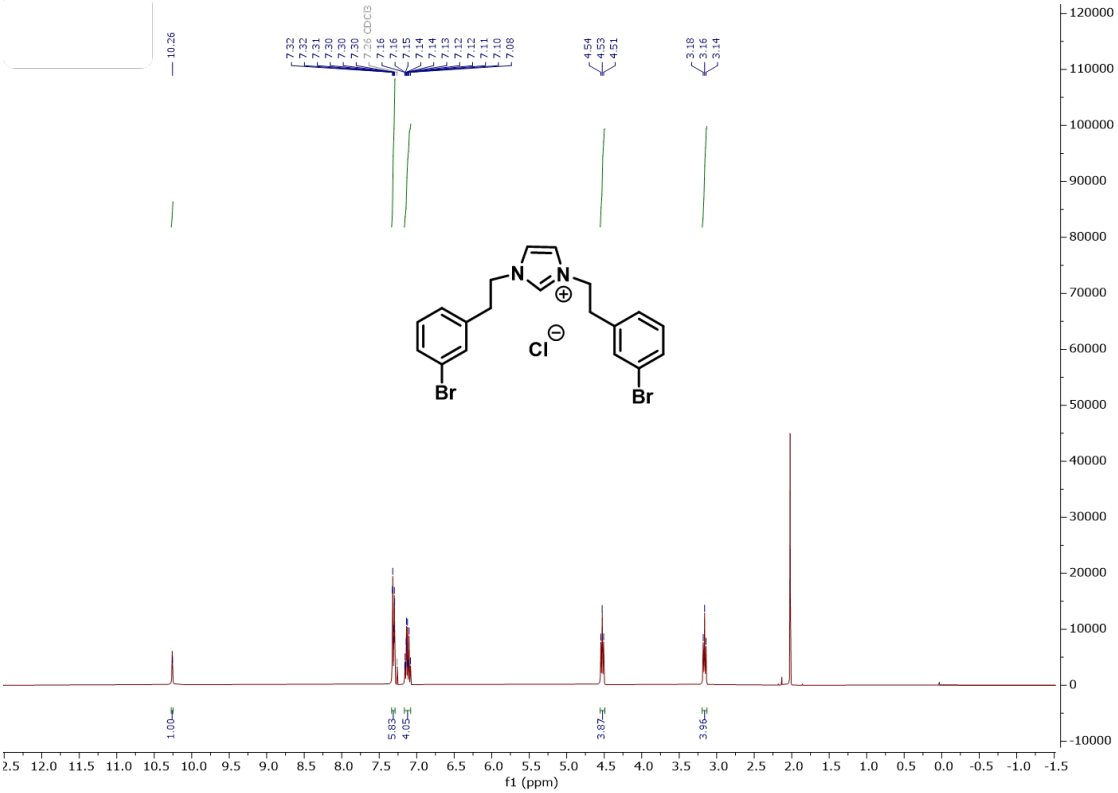

Figure S25: ^{1}H NMR of **1d**

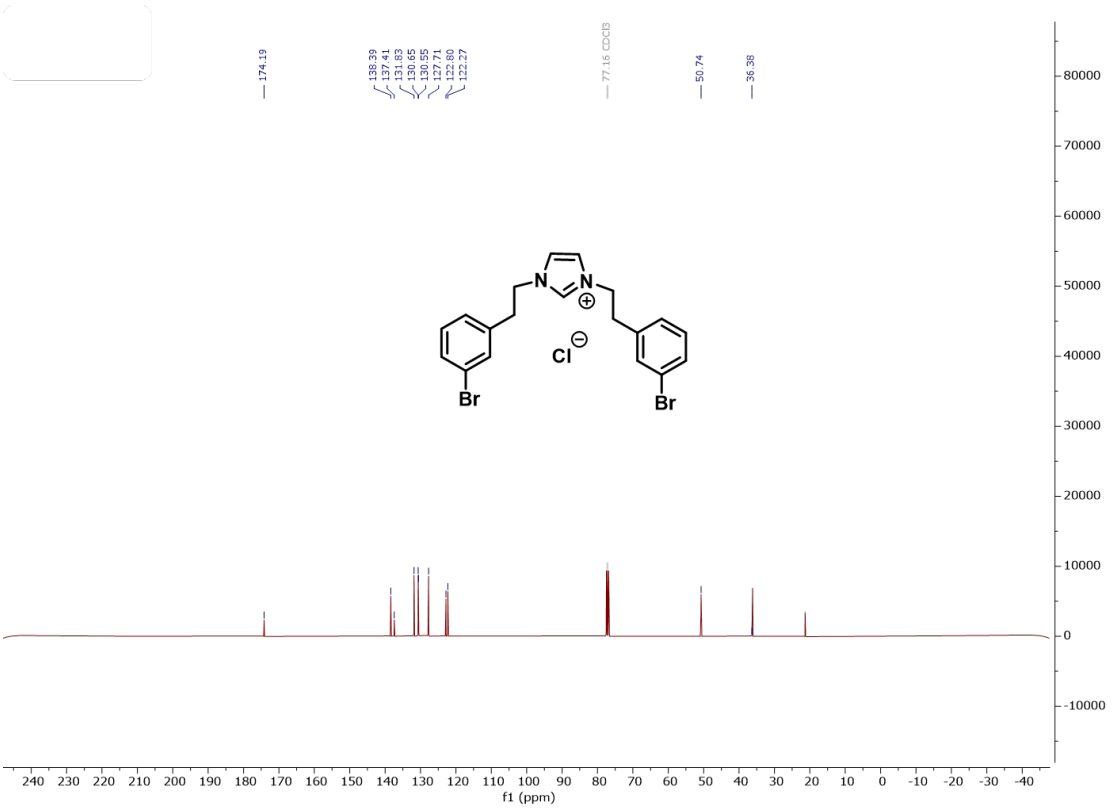

Figure S26: ^{13}C NMR of **1d**

1,3-Bis(2-bromophenethyl)-1*H*-imidazol-3-ium chloride (2d)

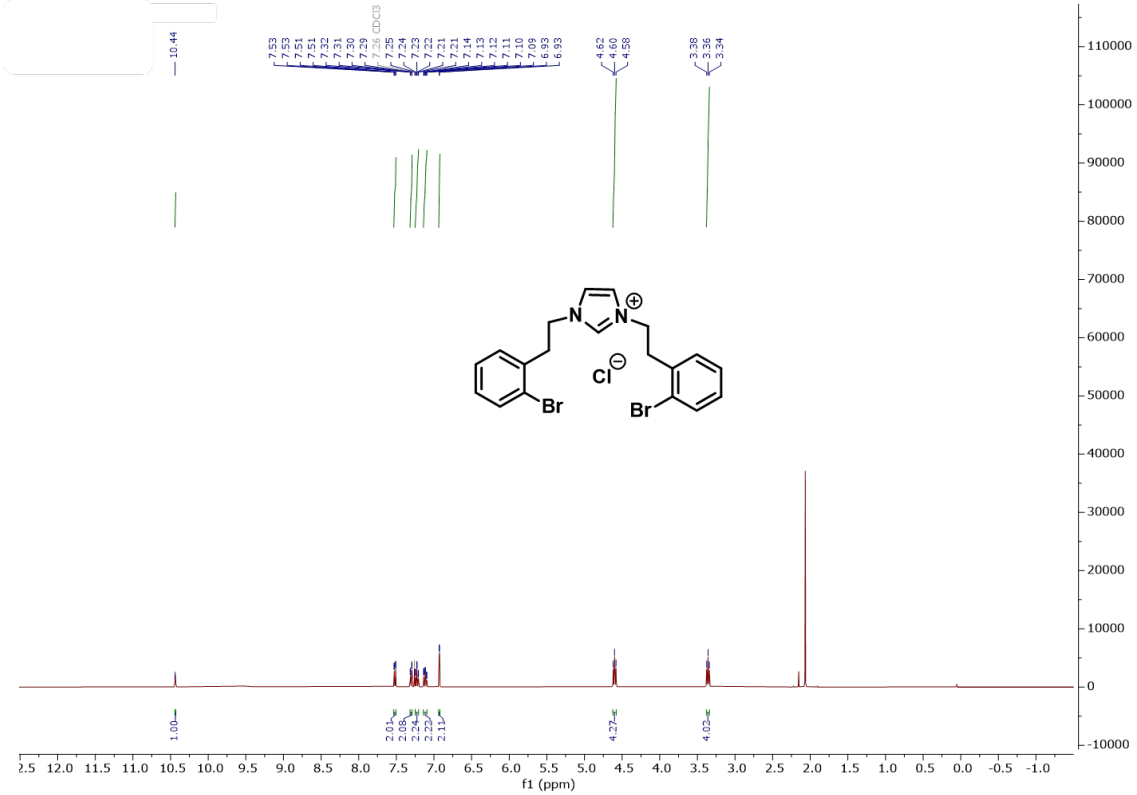

Figure S27: ^{1}H NMR of **2d**

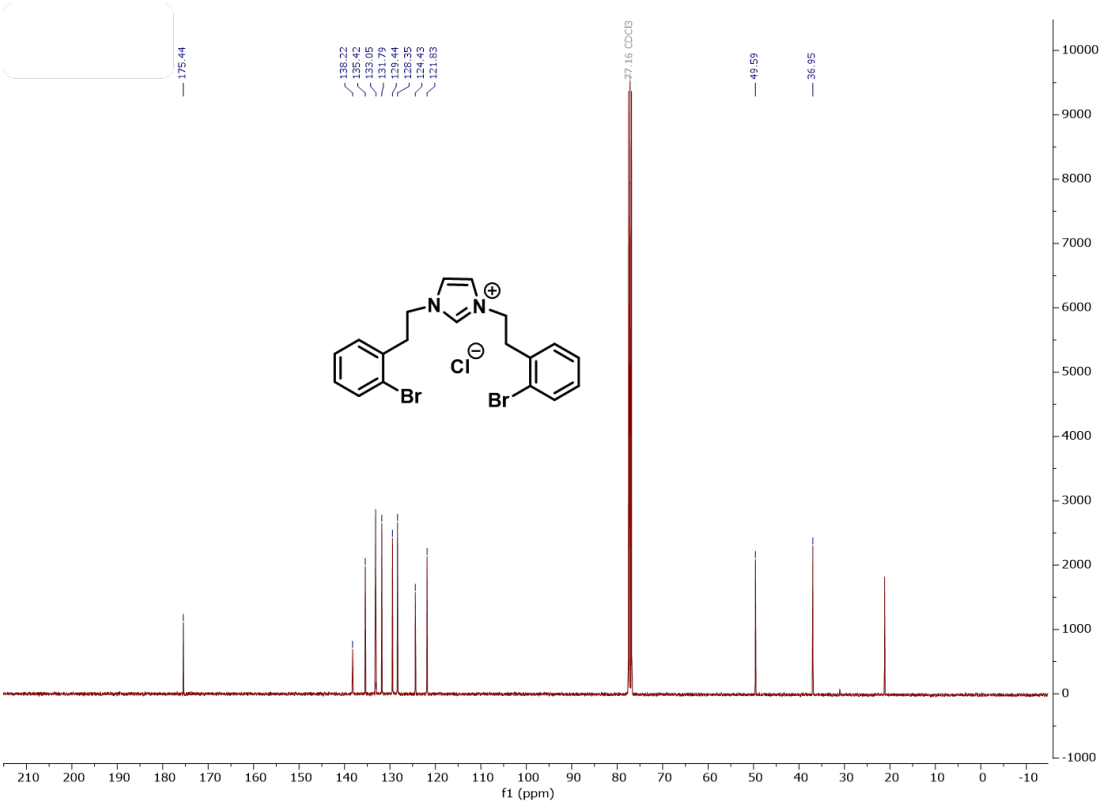

Figure S28: ^{13}C NMR of **2d**

1,3-Bis(4-bromophenethyl)-1*H*-imidazol-3-ium chloride (3d)

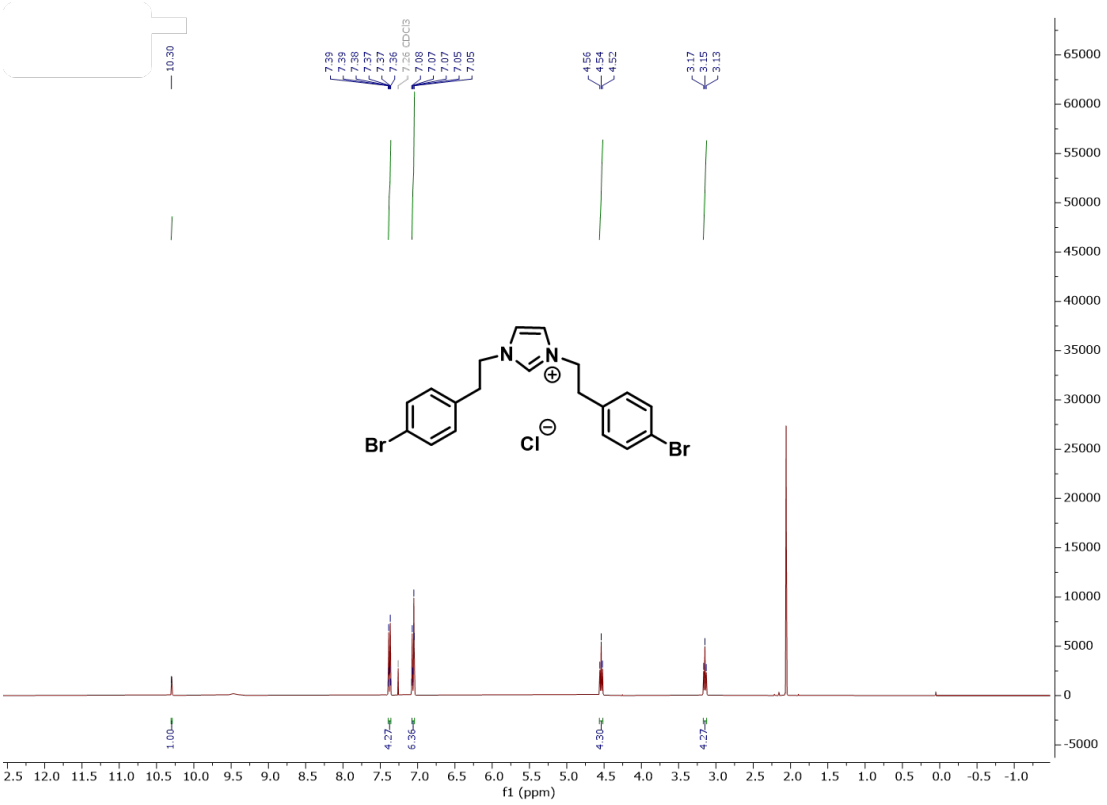

Figure S29: ^{1}H NMR of **3d**

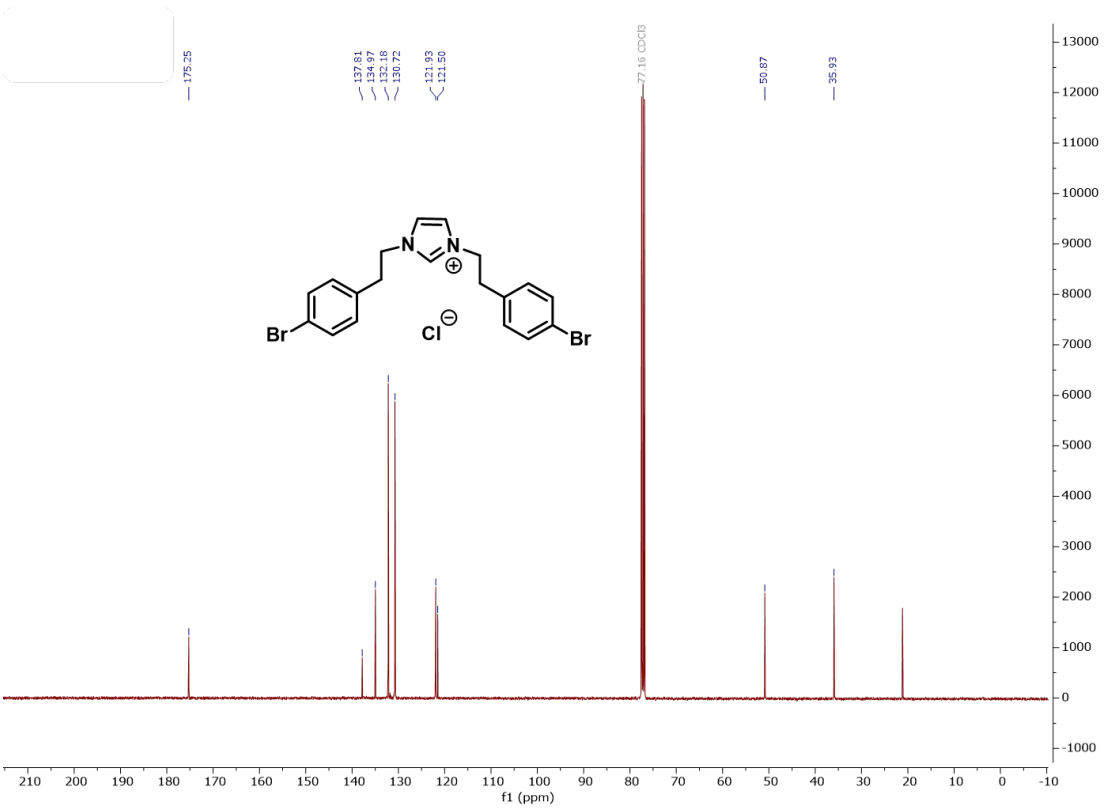

Figure S30: ^{13}C NMR of **3d**

1,3-Bis(3-chlorophenethyl)-1*H*-imidazol-3-ium chloride (4d)

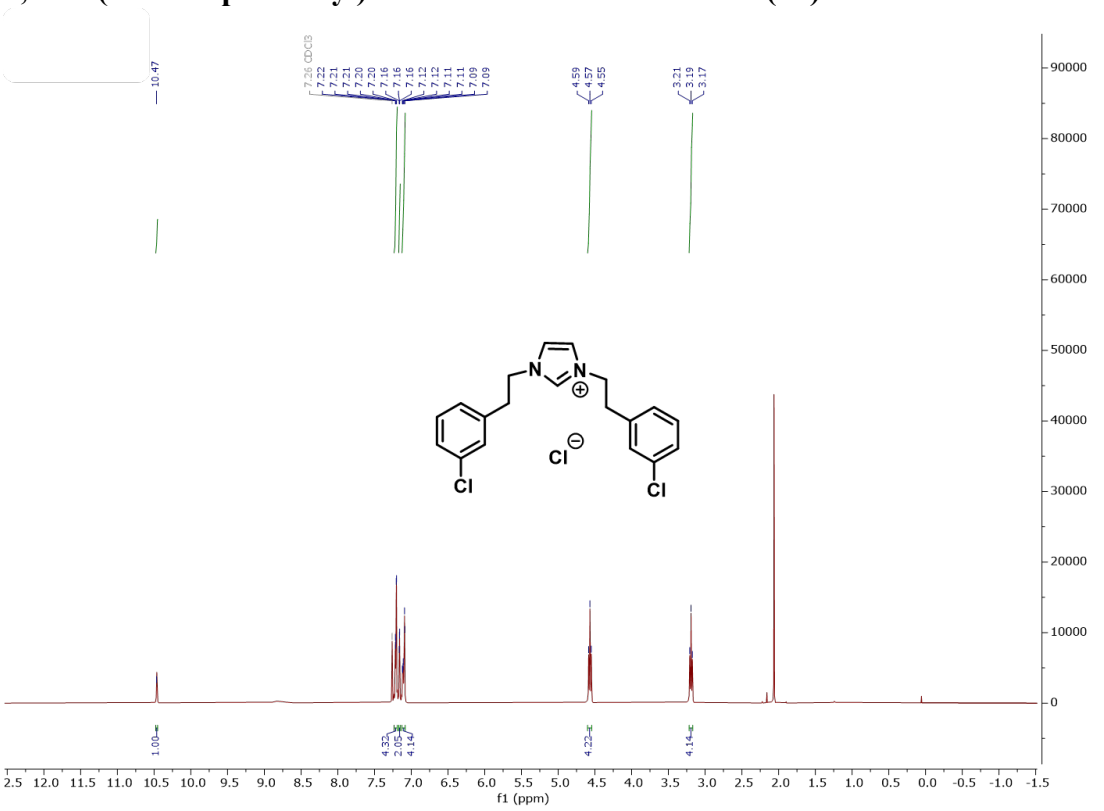

Figure S31: ^{1}H NMR of **4d**

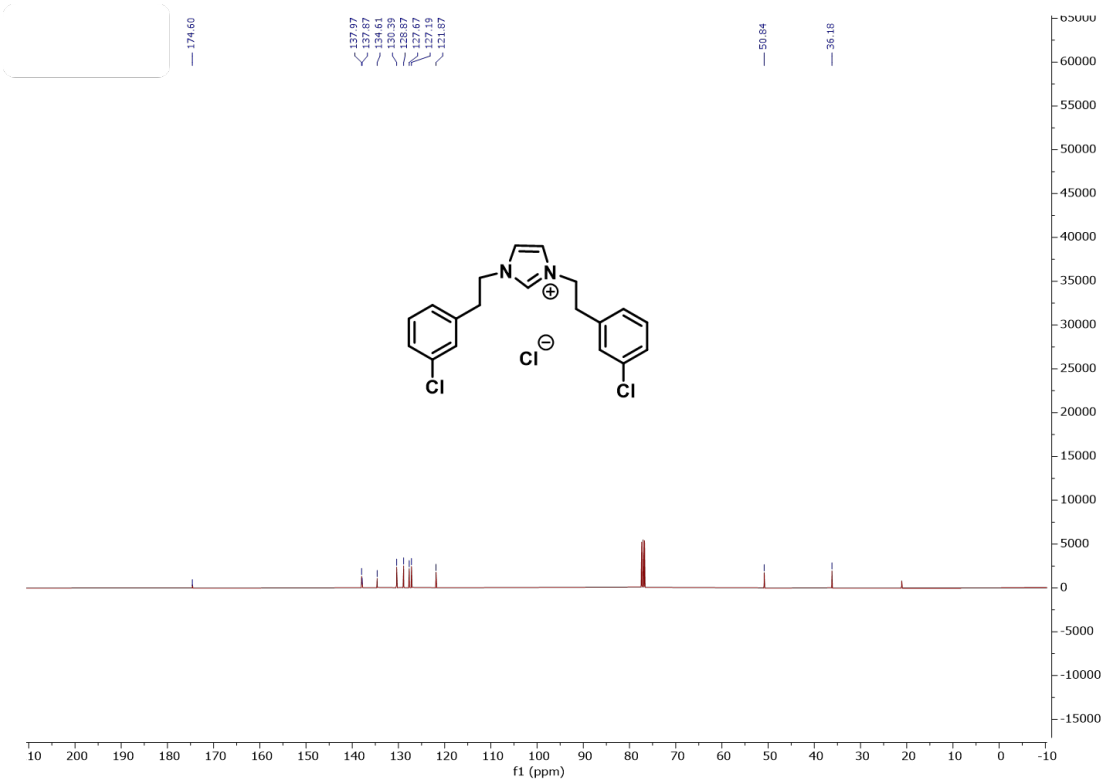

Figure S32: ^{13}C NMR of **4d**

1,3-Bis(3-iodophenethyl)-1*H*-imidazol-3-ium iodide (5d)

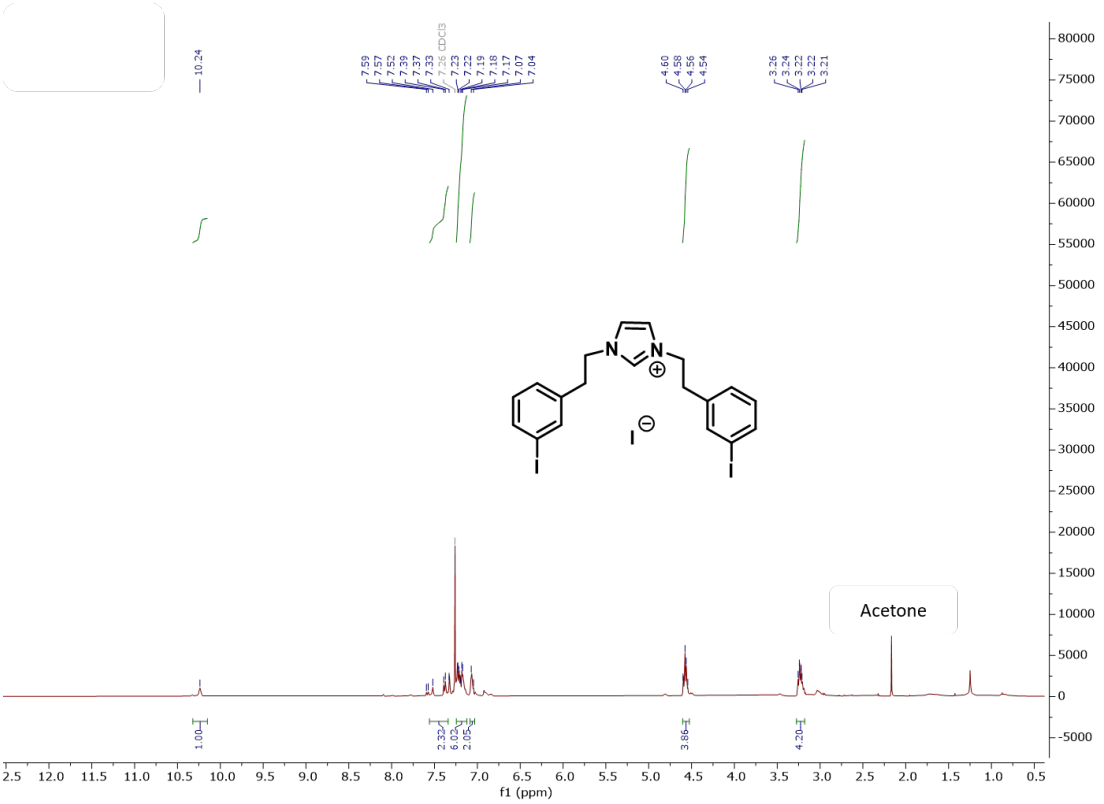

Figure S33: ^{1}H NMR of **5d**

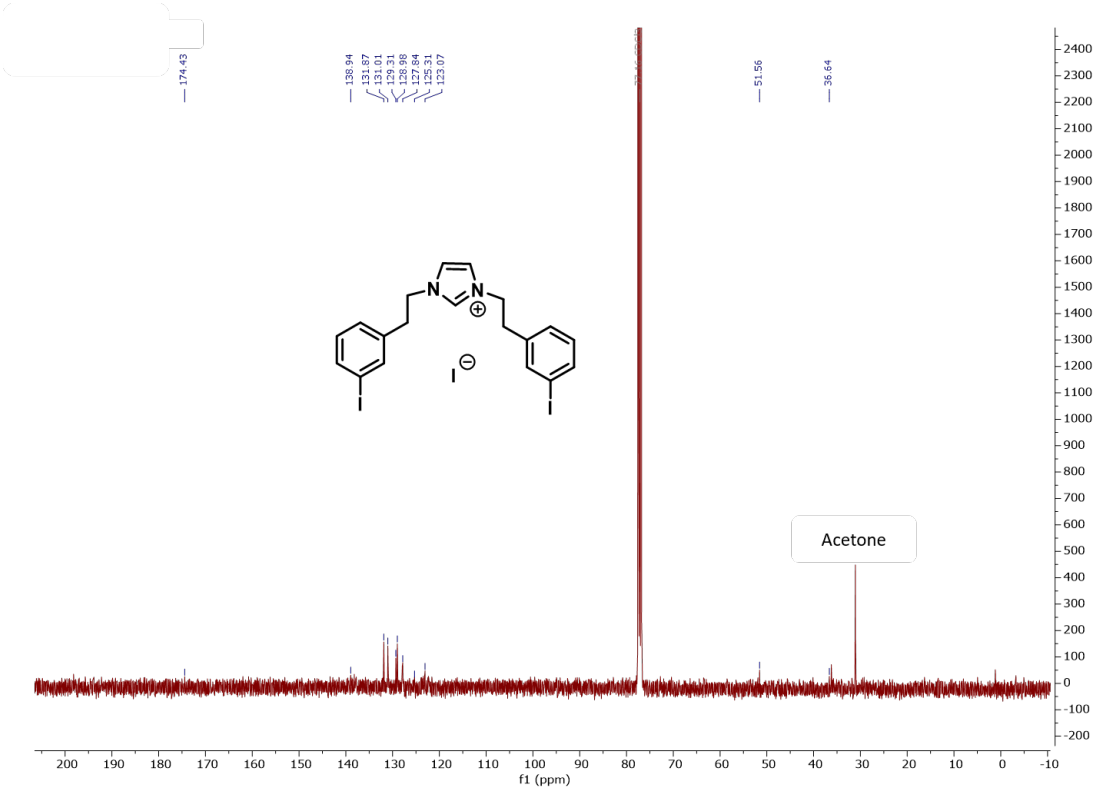

Figure S34: ^{13}C NMR of **5d**

***m*-(5-(3-Bromophenyl)pentyl)-1H-3λ^4-imidazole (6di)**

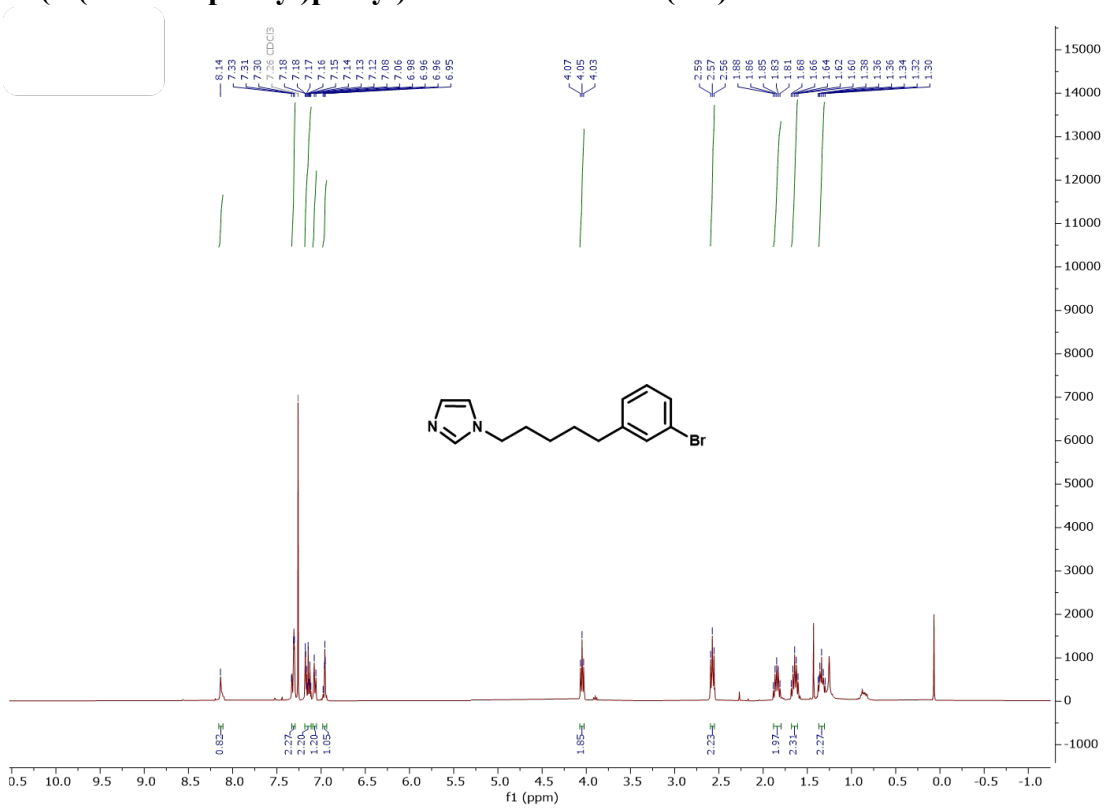

Figure S35: ^{1}H NMR of **6di**

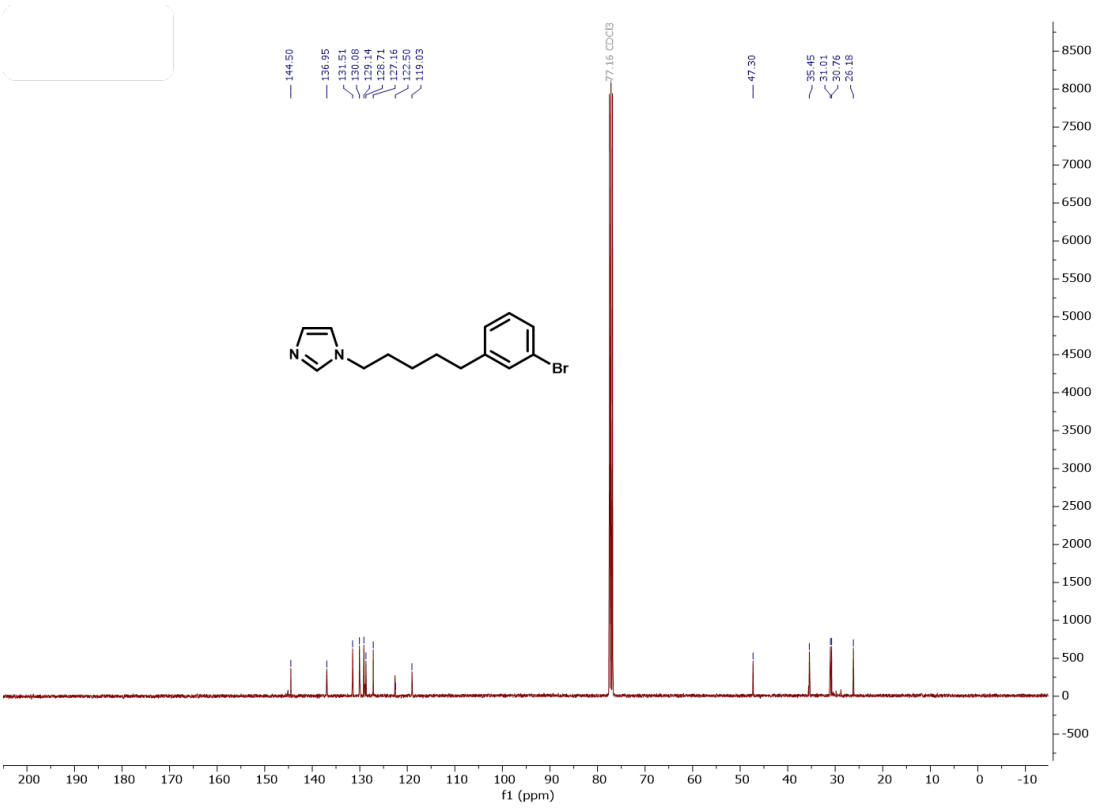

Figure S36: ^{13}C NMR of **6di**

1,3-Bis(5-(3-bromophenyl)pentyl)-1*H*-3λ^4-imidazole (6d)

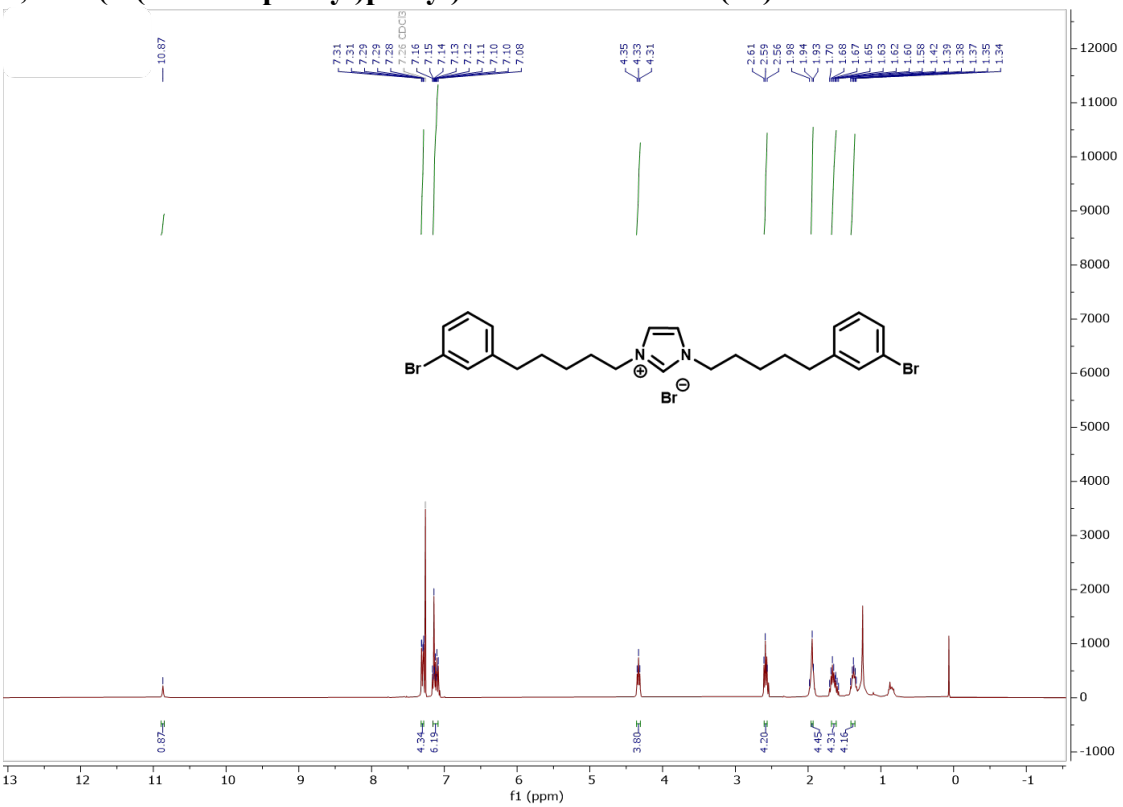

Figure S37: ^{1}H NMR of **6d**

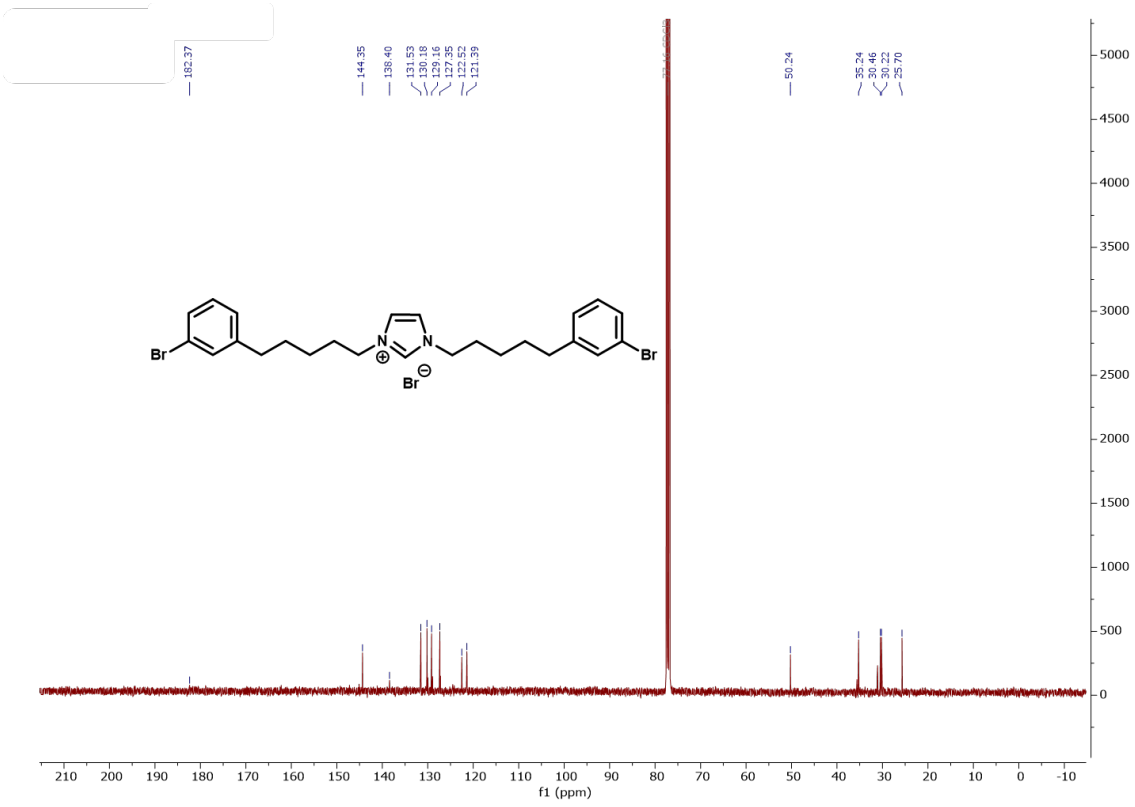

Figure S38: ^{13}C NMR of **6d**

(1,3-Bis(3-bromophenethyl)-2,3-dihydro-1*H*-imidazol-2-yl)gold(I) chloride (1e)

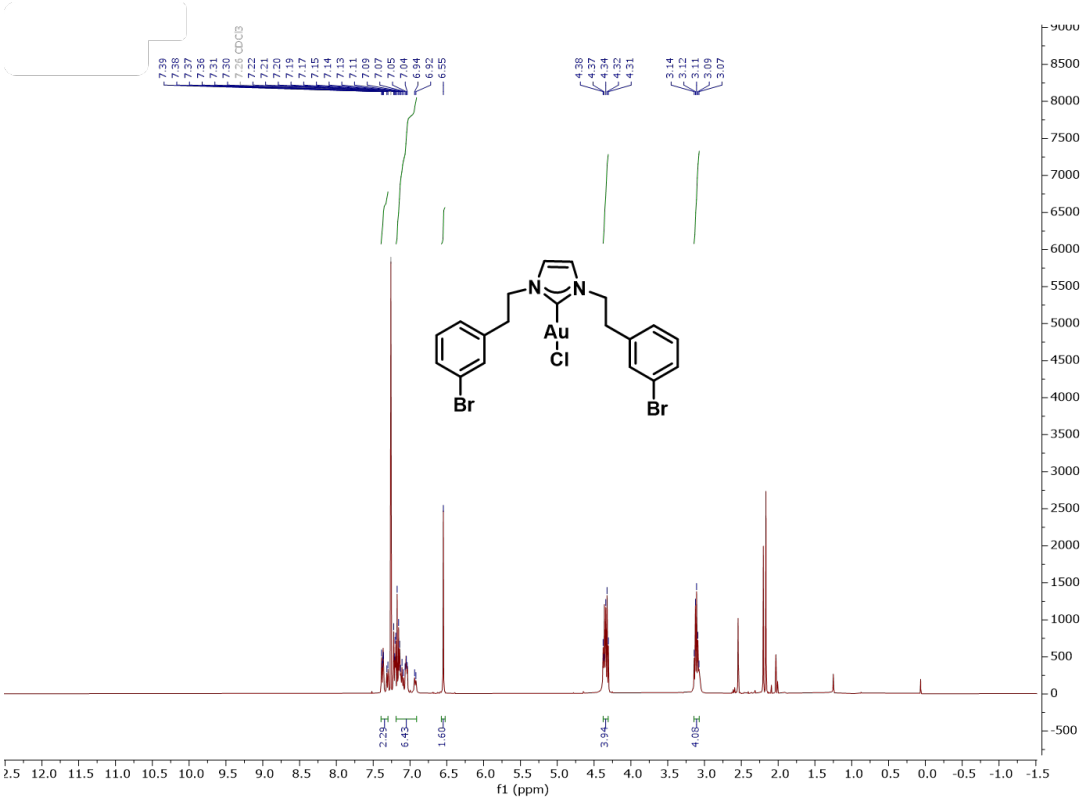

Figure S39: ^{1}H NMR of **1e**

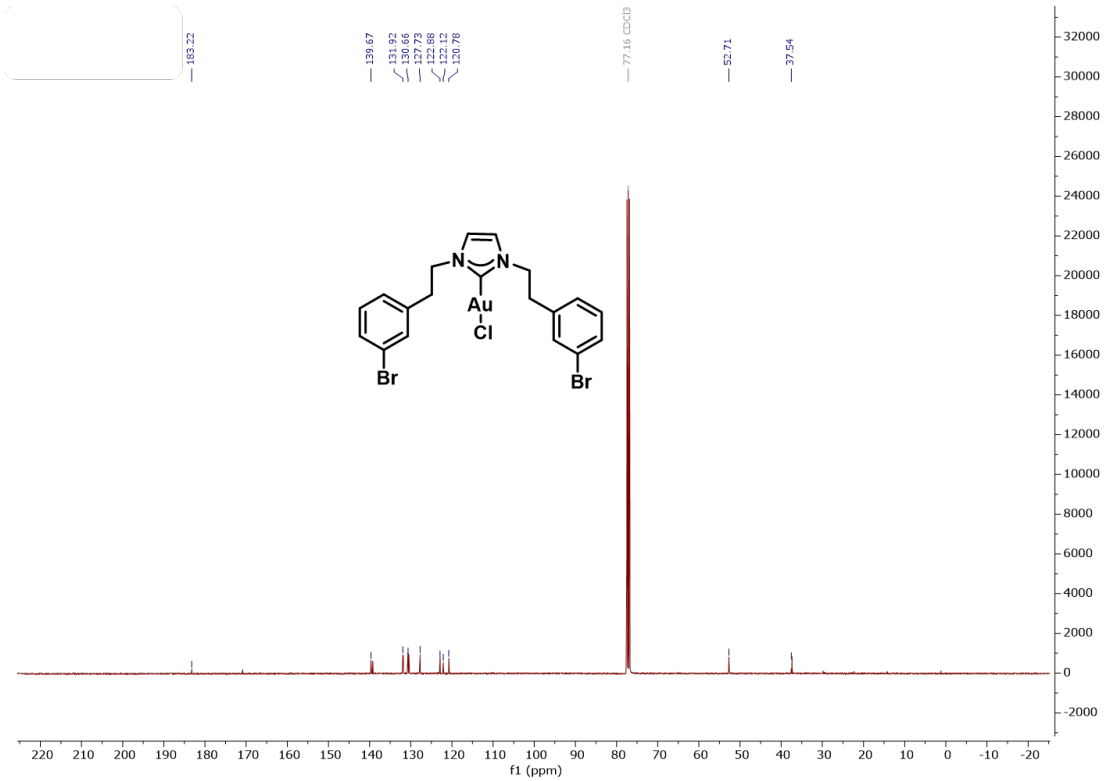

Figure S40: ^{13}C NMR of **1e**

(1,3-Bis(2-bromophenethyl)-2,3-dihydro-1*H*-imidazol-2-yl)gold(I) chloride (2e)

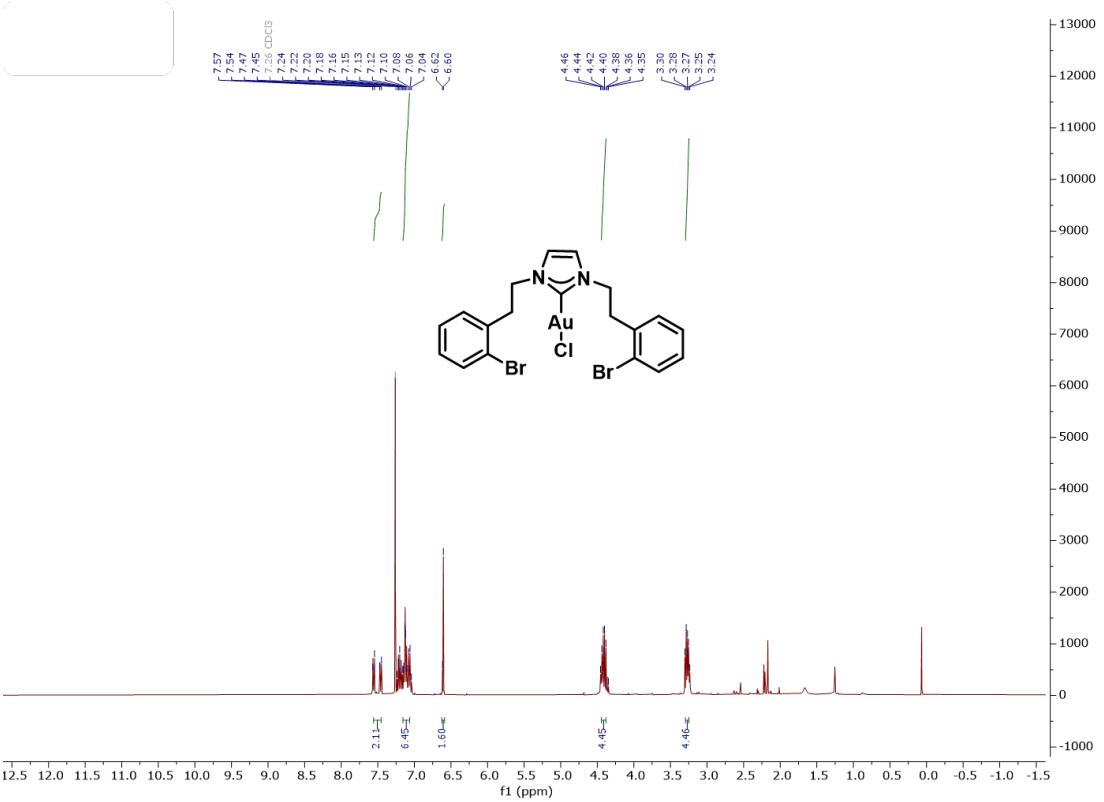

Figure S41: ^{1}H NMR of **2e**

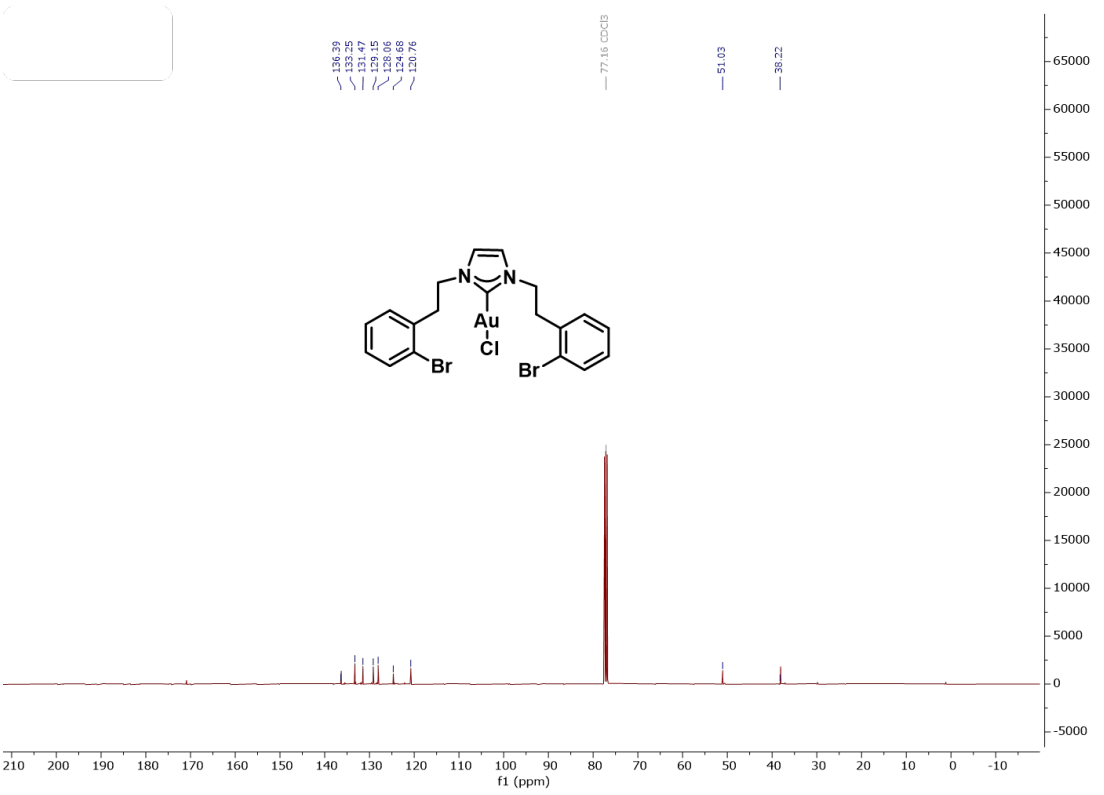

Figure S42: ^{13}C NMR of **2e**

(1,3-Bis(4-bromophenethyl)-2,3-dihydro-1*H*-imidazol-2-yl)gold(I) chloride (3e)

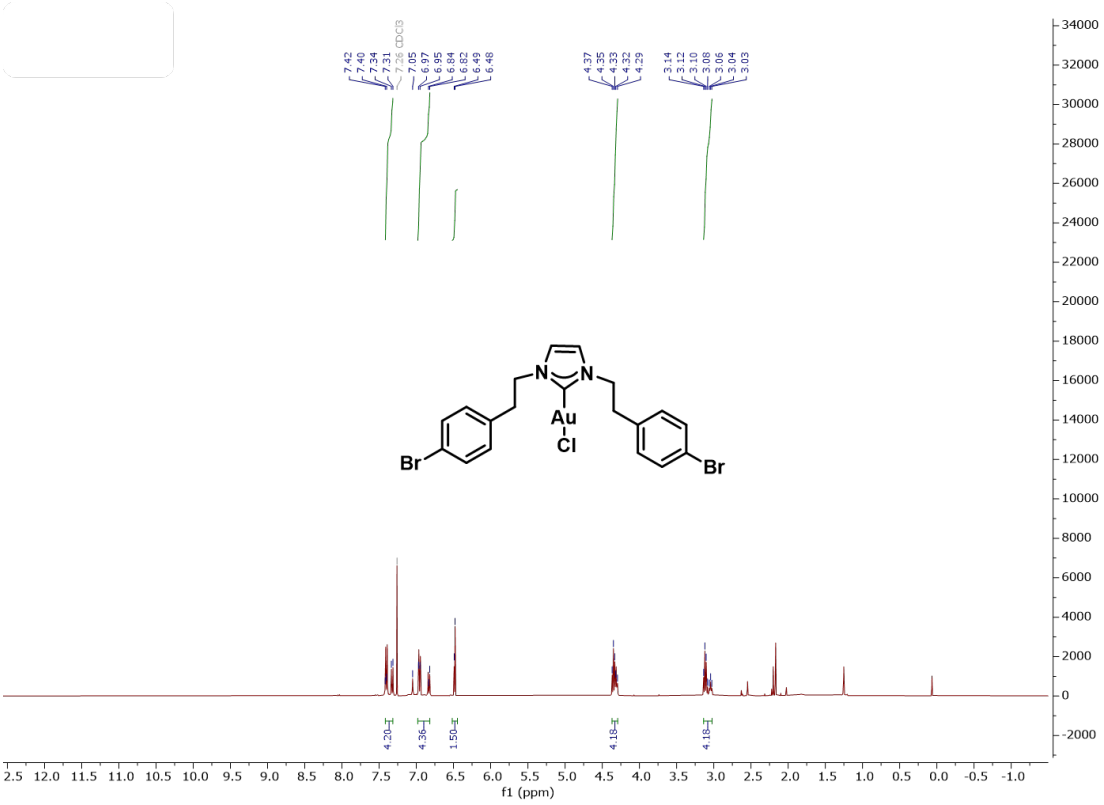

Figure S43: ^{1}H NMR of **3e**

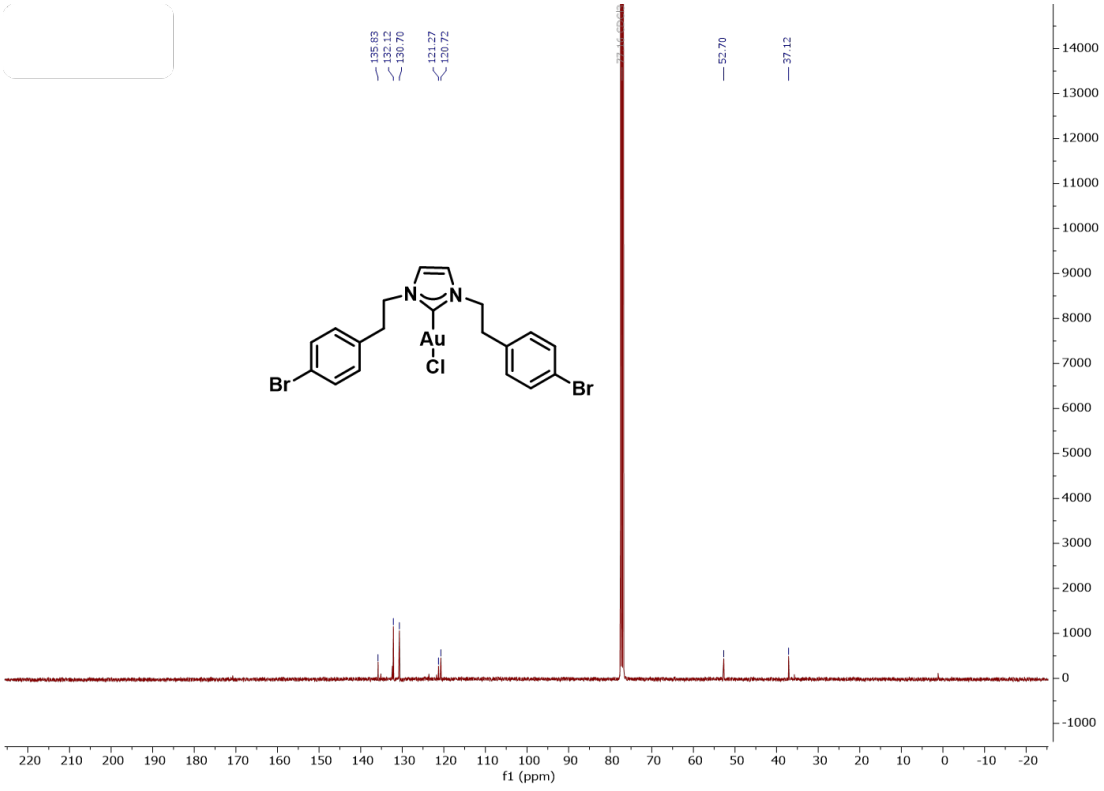

Figure S44: ^{13}C NMR of **3e**

(1,3-Bis(3-chlorophenethyl)-2,3-dihydro-1H-imidazol-2-yl)gold(I) chloride (4e)

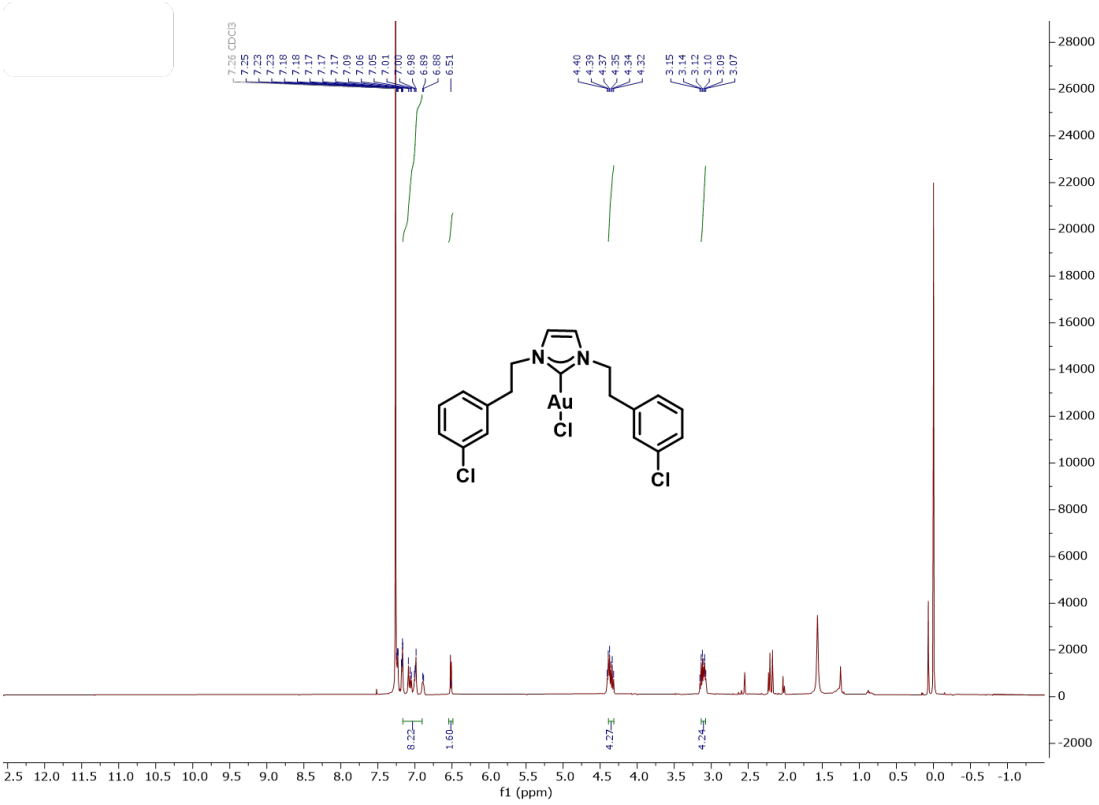

Figure S45: ^{1}H NMR of **4e**

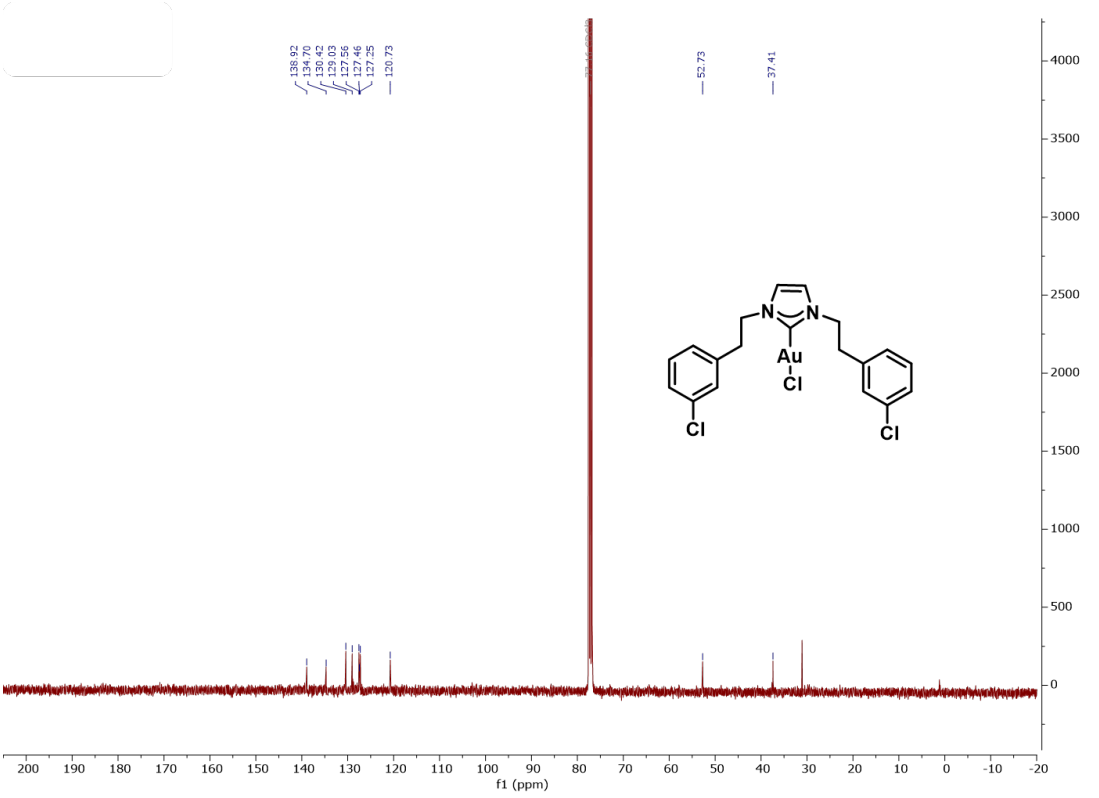

Figure S46: ^{13}C NMR of **4e**

(1,3-Bis(3-iodophenethyl)-2,3-dihydro-1*H*-imidazol-2-yl)gold(I) iodide (5e)

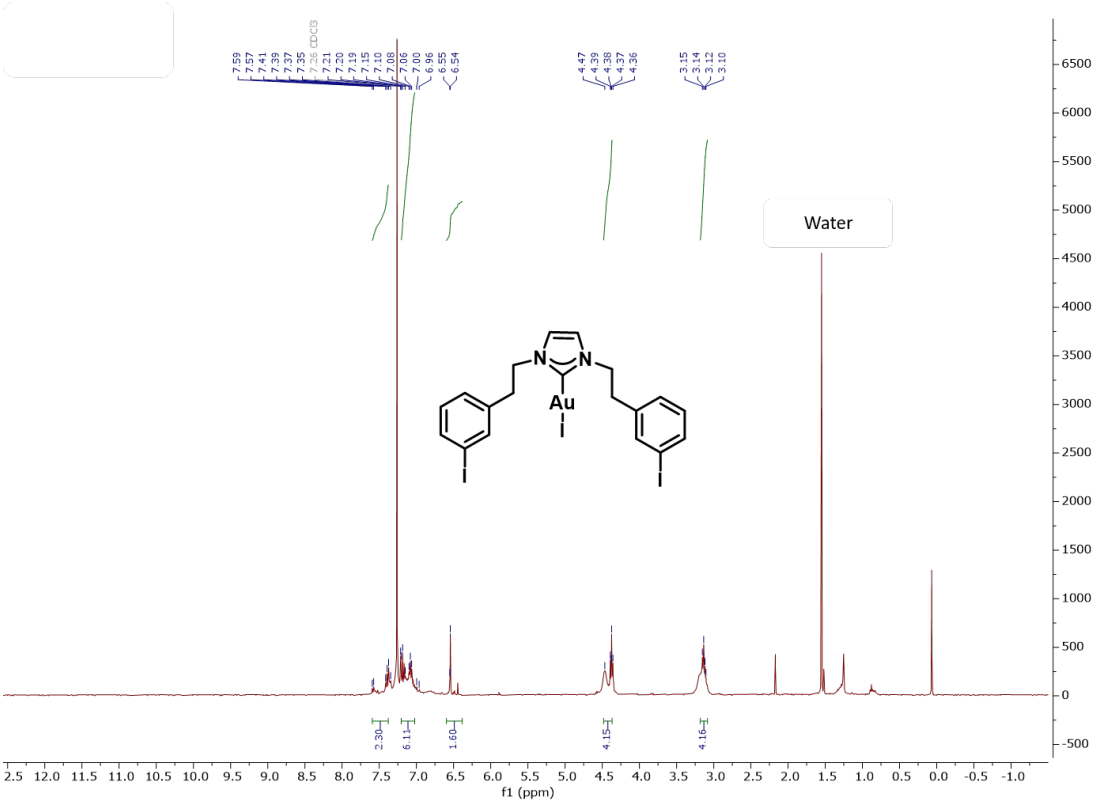

Figure S47: ^{1}H NMR of **5e**

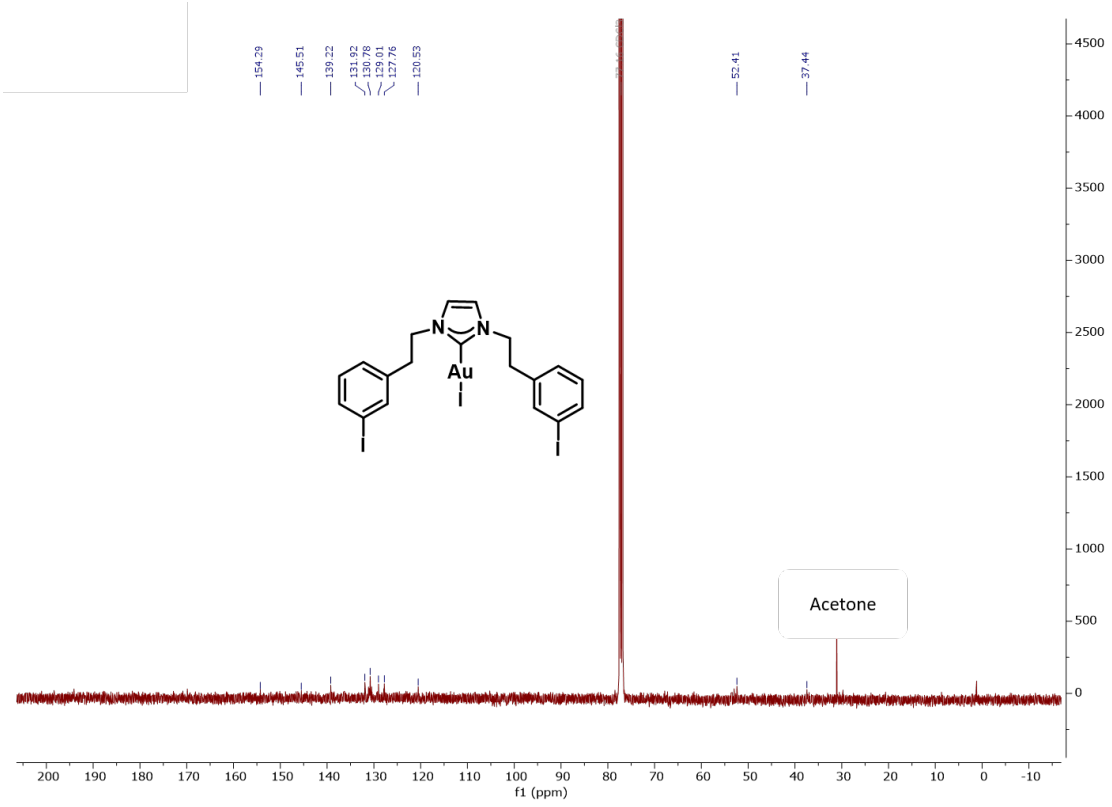

Figure S48: ^{13}C NMR of **5e**

(1,3-Bis(5-(3-bromophenyl)pentyl)-1*H*-3λ^4-imidazol-2-yl)gold(I) bromide (6e)

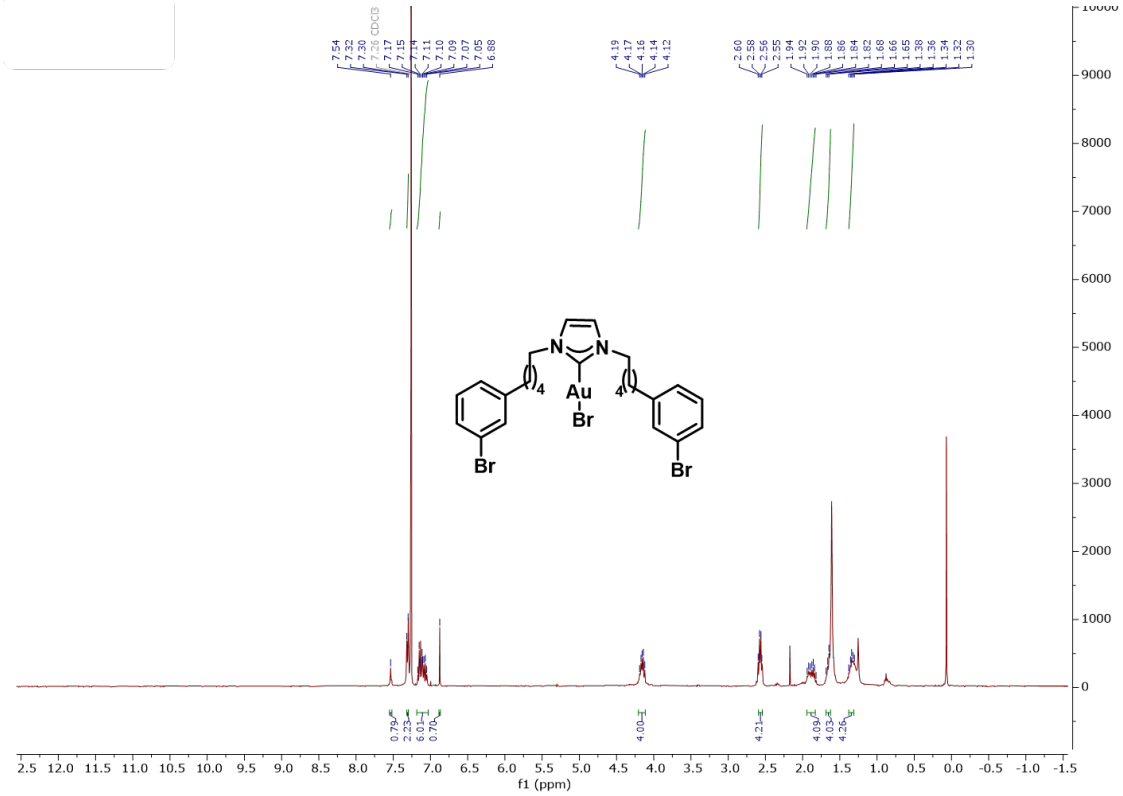

Figure S49: ^{1}H NMR of **6e**

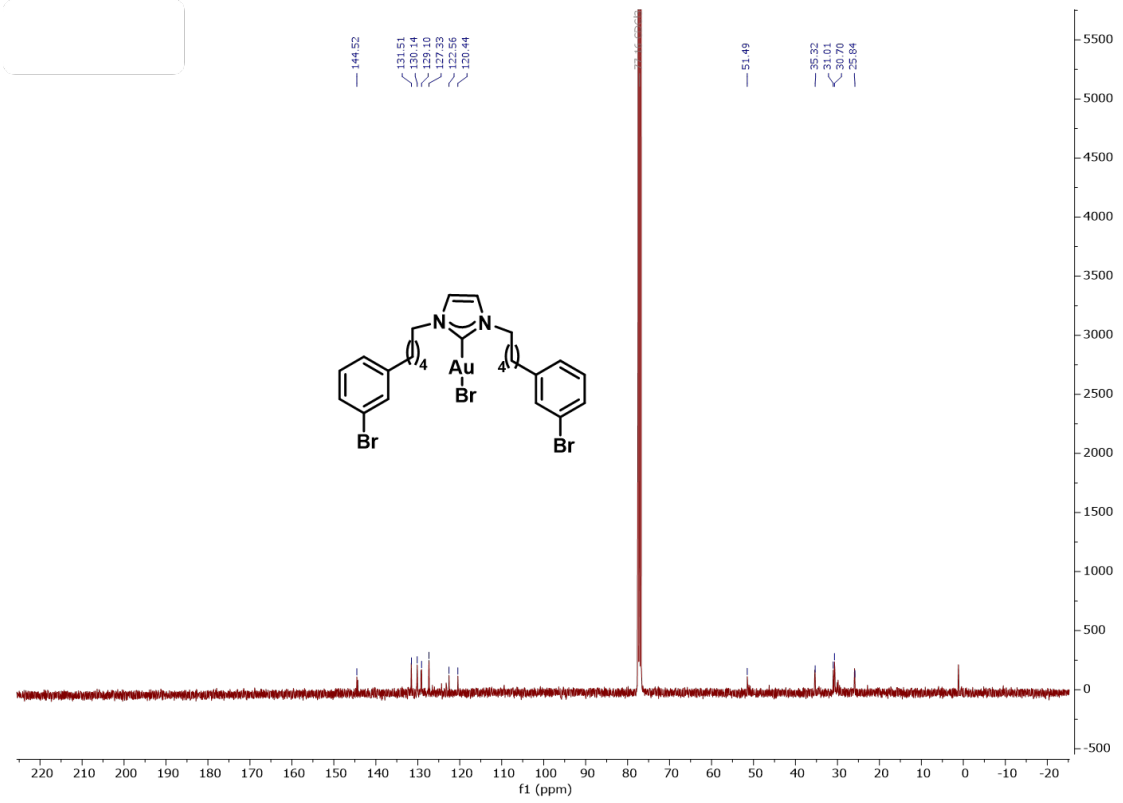

Figure S50: ^{13}C NMR of **6e**

References

1 G. R. Fulmer, A. J. M. Miller, N. H. Sherden, H. E. Gottlieb, A. Nudelman, B. M. Stoltz, J. E. Bercaw and K. I. Goldberg, NMR Chemical Shifts of Trace Impurities: Common Laboratory Solvents, Organics, and Gases in Deuterated Solvents Relevant to the Organometallic Chemist, *Organometallics*, 2010, **29**, 2176–2179.

2 M. H. Dunn, N. Konstandaras, M. L. Cole and J. B. Harper, Targeted and Systematic Approach to the Study of pKa Values of Imidazolium Salts in Dimethyl Sulfoxide, *J. Org. Chem.*, 2017, **82**, 7324–7331.

3 M. Bélanger-Bouliga, R. Mahious, P. I. Pitroipa and A. Nazemi, Perylene diimide-tagged N-heterocyclic carbene-stabilized gold nanoparticles: How much ligand desorbs from surface in presence of thiols?, *Dalton Trans.*, 2021, **50**, 5598–5606.

4 M. R. Narouz, C.-H. Li, A. Nazemi and C. M. Crudden, Amphiphilic N-Heterocyclic Carbene-Stabilized Gold Nanoparticles and Their Self-Assembly in Polar Solvents, *Langmuir.*, 2017, **33**, 14211–14219.

5 N. A. Nosratabad, Z. Jin, L. Du, M. Thakur and H. Mattoussi, N-Heterocyclic Carbene-Stabilized Gold Nanoparticles: Mono- Versus Multidentate Ligands, *Chem. Mater.*, 2021, **33**, 921–933.

6 S. K. Goetzfried, C. M. Gallati, M. Cziferszky, R. A. Talmazan, K. Wurst, K. R. Liedl, M. Podewitz and R. Gust, N-Heterocyclic Carbene Gold(I) Complexes: Mechanism of the Ligand Scrambling Reaction and Their Oxidation to Gold(III) in Aqueous Solutions, *Inorg. Chem.*, 2020, **59**, 15312–15323.

7 M. J. MacLeod and J. A. Johnson, PEGylated N-Heterocyclic Carbene Anchors Designed To Stabilize Gold Nanoparticles in Biologically Relevant Media, *J. Am. Chem Soc.*, 2015, **137**, 7974–7977.

8 C. Hirtenlehner, C. Krims, J. Hölbling, M. List, M. Zabel, M. Fleck, R. J. F. Berger, W. Schoefberger and U. Monkowius, Syntheses, crystal structures, reactivity, and photochemistry of gold(III) bromides bearing N-heterocyclic carbenes, *Dalton Trans.*, 2011, **40**, 9899–9910.

9 S. R. Thomas and A. Casini, N-Heterocyclic carbenes as “smart” gold nanoparticle stabilizers: State-of-the art and perspectives for biomedical applications, *J. Organomet. Chem*, 2021, **938**, 121743.

10 G. Li, C. Liu, Y. Lei and R. Jin, Au25 nanocluster-catalyzed Ullmann-type homocoupling reaction of aryl iodides, *Chem Comm*, 2012, **48**, 12005–12007.